



A chemical examination of faience found in Nubia: preliminary observations

Juliet V. Spedding

University of Liverpool, 14 Abercromby Square, Liverpool L69 7WZ, UK

ARTICLE INFO

Keywords:

Nubia
Faience
SEM-EDS
Kerma
Faras
Meroe
Sanam
Kawa
Vitreous Materials

ABSTRACT

Egyptian faience has been extensively studied, while faience found in Nubia has received little attention. This pilot study uses scanning electron microscopy with energy dispersive spectrometry (SEM-EDS) to examine 30 faience samples (bead and vessel fragments) from sites in Lower Nubia (Faras) and Upper Nubia (Kerma, Kawa, Sanam, Meroe) dated from the C-Group to the Meroitic Period (c.2160BC–AD350). The findings show the varied quality of the production of faience from Nubia with the potential identification of the use of cementation glazing in C-Group material, the presence of ‘glassy faience’ at Kerma, and the presence of high lead levels in a Napatan Period sample. The discussion that follows highlights the potential innovation in the development of faience found in Nubia set in the wider historical/social/political context. These results highlight the need for further examination of this vitreous material when found in Nubia and how it might have developed alongside—and separately from—faience found in Egypt.

1. Introduction

1.1. Geographical and Archaeological context

Nubia (ancient Sudan) refers to the geographical region south of Aswan, Egypt, that at its largest extended to the Sixth Cataract (see Fig. 1). Like its northern neighbour, Nubia can be referred to as Lower Nubia (north) and Upper Nubia (south). Over the time periods spanned by the material examined here—from the C-Group Phase Ia (c.2160–2055BC) to the Meroitic Period (c.350BC–AD350)—Nubia would see many different ruling powers and cultures: the Kingdom of Kerma (c.2050–1450BC), the Napatan kings (c.750–350BC) who would also rule Egypt (25th Dynasty (747–656BC)), and the later, powerful, Meroitic Kingdom (c.350BC–AD350). (See Table 1 for the Lower and Upper Nubian chronologies used here and how they relate to Egyptian chronology (see Török, 2009; Minor 2012; 2014 for Middle and Classic Kerma Period dates)).

This pilot study examines 30 faience bead and vessel samples with a known provenance of Faras from Lower Nubia, and from the Upper Nubian sites of Kerma, Kawa, Sanam, and Meroe. The samples date from the C-Group Phase Ia to the Meroitic Period (c.2160BC–AD350). This study was undertaken in order to assess the composition and glazing methods of faience found in Nubia with the aim of presenting an initial overview of the compositions and development of this vitreous material

within that region. Egyptian faience has been more extensively studied than that from Nubia, so it is the compositional details and the glazing methods of Egyptian faience that will first be discussed. The materials and methods for analysing these samples will then be presented and the chemical results given, followed by a discussion of these results with particular focus on the potential identification of glassy faience at Kerma. The presence of unusually high lead levels in a Napatan Period sample from Sanam is also discussed.

1.2. Egyptian faience

Faience production in Egypt has an extensive history and the technological processes developed over time (see for example Nicholson et al., 2009; Kaczmarczyk and Hedges, 1983; Lucas and Harris, 1962). Regarding Egyptian faience, it is first attested during the Badarian Culture (c.5500–4000BC) (Stocks, 1997), making it the first known man-made non-clay ceramic (Nicholson et al., 2009). In Nubia this time period covers different cultural phases that have been assigned based on ceramic finds and includes the El Baqar (c.5400–4700BC) and El Ansam (c.4600–3500BC) in the Nabta-Kiseiba Region, the KV2b,c (c.5600–5000BC) to Abkan (c.5000–4000BC) in the Lower Nubia region, material from Cemetery R12 at Kawa (c.4800–4200BC) in the Kerma Seleim Basin, and Multaga/Kurat (c.5000–4000BC) in the Fourth Cataract and Dongola Reach regions (see Gatto, 2011 for further details

E-mail address: julietvspedding@gmail.com.

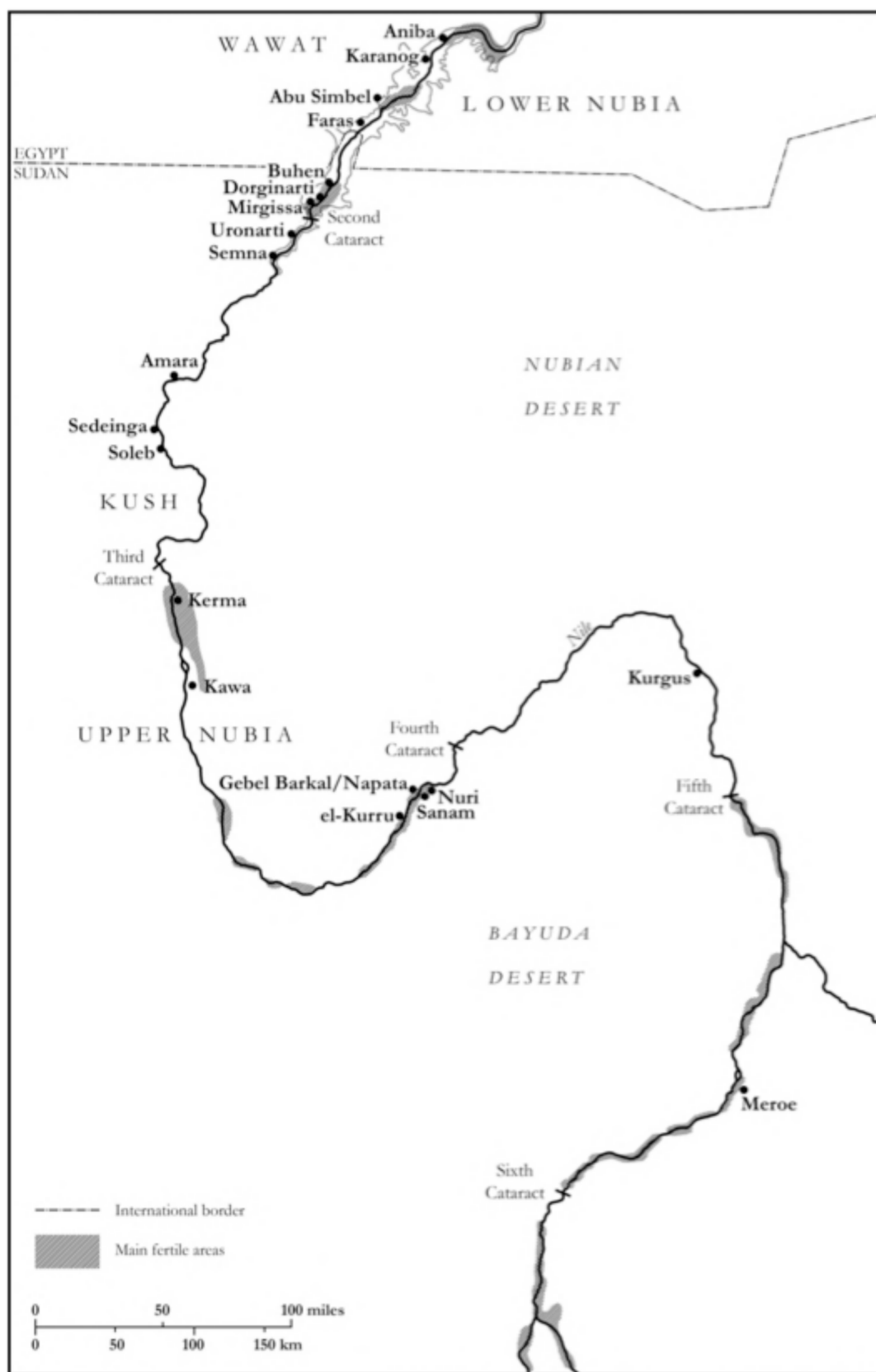


Fig. 1. Map of Nubia with key sites from the time periods shown (map by D. Probert).

Table 1

Timeline of Lower Nubia, Upper Nubia, and Egypt.

LOWER NUBIAN TIME PERIOD(S)	DATE	UPPER NUBIAN TIME PERIOD(S)	DATE	EGYPTIAN TIME PERIOD(S)	DATE
C-Group Phase Ia	c.2350– 2055BC	Old Kerma	c.2450– 2050BC	First Intermediate Period	c.2160– 2055BC
C-Group Phase Ib– IIa	c.2055– 1650BC	Middle Kerma	c.2050– 1700BC	Middle Kingdom	c.2055– 1650BC
		Classic Kerma	c.1700– 1550BC	Middle Kingdom/Second Intermediate Period/Start of New Kingdom	c.2055– 1550BC
C-GROUP VANISHES	AFTER C.1500BC	KERMA KINGDOM ENDS	C.1550BC	NEW KINGDOM	c.1550– 1069BC
Napatan Period				Third Intermediate Period (21 st –24 th Dynasties)	c.1069– 747BC
Meroitic Period				Third Intermediate Period (Nubian 25 th Dynasty)	c.747– 646BC
c.747–350BC				Late Period	c.664BC–332BC
c.350BC–AD350				Ptolemaic Period	332–30BC
				Roman Period	30BC– AD394

and full discussion of the relative chronology of Nubia up to c.2600BC).

Faience consists of a ground-quartz paste body with an alkaline glaze (Tite et al., 1983). Vandiver (1982) identified the typical body composition of Egyptian faience as 92–99 % SiO₂ (silica), 1–5 % CaO (lime), 0.5–3 % alkali/Na₂O (soda) and minor amounts of CuO (copper oxide), Al₂O₃ (aluminium oxide), TiO₂ (titanium oxide), MgO (magnesia/magnesium oxide), K₂O (potassium oxide), and Fe₂O₃ (iron (II) oxide) (Hammerle, 2011).

Desert sand is believed to be the most likely source of the silica, identifiable chemically by the presence of impurities such as chalk, limestone, or iron, there is also the potential for crushed quartz pebbles to have been used instead (Nicholson et al., 2009). Other impurities, albeit in tiny amounts, could also be introduced through the grinding tools used (Rehren, 2008). Another possible source for the body material is the waste products from stone-working using copper drills (Stocks, 1997).

The 0.5–3 % of alkali could come from two main sources – from the mineral natron or from certain halophytic plants that when burnt yield either potash (identifiable by the higher value of magnesia) or soda (Nicholson et al., 2009). There is also the possibility, like in glass making, that lead (detected as PbO) could have been added as a flux (Rehren and Freestone, 2015), something potentially seen in the faience examined here (see below). The presence of up to 5 % CaO is either accidental, found in desert sand used as a silica source, or a deliberate addition when crushed quartz pebbles were used (Nicholson et al., 2009). The remaining very small amounts of the constituents of faience are present through accidental inclusion of ‘contaminated’ raw materials or deliberate additions made to colour the glaze (Nicholson et al., 2009).

Following the primary production stage during which the raw materials were processed, the resulting paste was then shaped. The method for shaping would develop over faience’s long history and could be done by modelling the core, freeform modelling, core forming, pressing into an open-face mould, or even throwing like a potter would on a wheel (Nicholson et al., 2009). This core would then be glazed by either efflorescence, cementation, or application (see Table 2), and then fired. The firing range was from 800 to 1,000 °C although the use of charcoal as a heat source is debated (Nicholson et al., 2009). During firing the objects could have been protected from smoke and ash, with those being glazed by efflorescence or application possibly placed on trays or saggars, with lids to protect them. For cementation glazing the object would be buried in the glazing powder inside a receptacle. These receptacles may have been high in alumina to help prevent the contents from sticking. While the exact nature of these receptacles is unknown, small marl-clay balls and annuli found at Lisht may have served this purpose (Nicholson et al., 2009).

Whilst Tite and Shortland (2008) and Nicholson et al. (2009) mention very little interstitial glass as a result of the cementation glazing technique, Matin and Matin (2012; 2016) have shown, through experimental archaeology, the potential for interstitial/interparticle glass in cementation glazing. In light of this, the results below will consider cementation glazing as a possibility alongside efflorescence glazing when there is both a decrease in the level of the identified colourant even when interparticle glass is observed.

2. Materials and methods of this study

Of the 30 samples examined here (see Table 3 for full details), 24

Table 2

Faience glazing techniques (Information from Nicholson et al., 2009; Tite and Shortland, 2008).

Glazing technique	Description	Process
Efflorescence	Self-glazing method	Glazed materials as soluble salts mixed with raw crushed quartz and alkalis of body material. Water in body evaporates and salts migrate to the surface of the object to form a crust. Precipitated salts comprise sodium-carbonates and to a smaller degree potassium-carbonates, sulphates, and chlorides. Concentration of copper is constant throughout the sample. In firing this layer melts and fuses to leave a glaze – thickness varies according to amount of efflorescence developed in drying. Rapid drying = greatest thickness. Interaction zone is generally narrow and well-defined. Presence of interstitial/interparticle glass in body of faience.
Cementation or 'Qom technique'	Self-glazing method	Artefact buried in glazing powder with a high flux content inside a vessel. Vessel and contents heated, powder becomes fused to the object by a chemical reaction between it and the surface of the object. Exact nature of this process not fully understood. Glaze appears uniform and concentration of copper rapidly decreases away from the surface. Interaction zone is thick and well-defined.
Application	Slurry applied to glaze core	Very little interstitial/interparticle glass in body of faience. Glazing materials – silica, lime, alkali – ground to small particle size, mixed with water to form a slurry. These materials may be ground together in their raw state or partially fritted and then ground as in production of pottery glaze. Fritting permits materials to react together, which helps the final firing temperature to be lower. Objects can be dipped or slurry poured over. Brushing is also possible. Glaze varies in thickness. A tendency to run and drip leads to pooling on the lower surfaces and thicker glazes on bases. Interaction zone is not well-defined. Very little interstitial/interparticle glass in body of faience.

came from the Manchester Museum and six from The Garstang Museum of Archaeology, Liverpool. Of the 24 from Manchester, two date to the C-Group Phase Ia Period, six to the Classic Kerma Period, three to the New Kingdom, nine to the Napatan Period, and four samples to the Meroitic Period. This material was excavated by Griffith with the C-Group Phase Ia samples, the New Kingdom material, and the Meroitic Period material all recovered from the Lower Nubian site of Faras (Griffith, 1921; 1924; 1925; 1926). Griffith also excavated at Sanam and Kawa in Upper Nubia,

with four of the nine Napatan Period samples coming from Kawa whilst the remaining five Napatan samples came from the cemetery at Sanam (Griffith, 1922; 1923).

The six samples of the Classic Kerma Period (c.1750–1450BC) material were recovered by Reisner (Reisner, 1923) from the Upper Nubian site of Kerma, Tumulus KX. See Minor (2012) for a discussion on the dating of Tumulus KX. This was the centre for the Kingdom of Kerma that rose to prominence at this time, remaining until the beginning of the

Table 3

Dataset of Nubian faience examined here (see Appendix Table A1–Table A5 for full details and images and Appendix Table A6 for all backscatter electron (BSE) images).

Accession and sample no.	Location	Provenance	Date	Colour	Description
MAN8439(a).1	Faras	C-Group Cemetery	C-Group Phase 1a	Pale green/blue exterior	Ring-shaped bead
MAN8439(a).2	Faras	C-Group Cemetery	C-Group Phase 1a	Pale green/blue exterior	Ring-shaped bead
MAN8561.1	Kerma	Tumulus KX	Classic Kerma	Dark turquoise	Ring-shaped bead
MAN8561.2	Kerma	Tumulus KX	Classic Kerma	Dark turquoise	Ring-shaped bead
MAN8561.3	Kerma	Tumulus KX	Classic Kerma	Dark turquoise	Ring-shaped bead
MAN8561.4	Kerma	Tumulus KX	Classic Kerma	Dark turquoise	Ring-shaped bead
MAN8561.5	Kerma	Tumulus KX	Classic Kerma	Dark turquoise	Ring-shaped bead
MAN8561.6	Kerma	Tumulus KX	Classic Kerma	Dark turquoise	Ring-shaped bead
MAN8442(a-e).3	Faras	Temple of Hathor	New Kingdom	Grey/green	Vessel fragment
MAN8442(a-e).4	Faras	Temple of Hathor	New Kingdom	Grey and red/brown	Vessel fragment
MAN8442(a-e).5	Faras	Temple of Hathor	New Kingdom	Light grey	Vessel fragment
MAN9341.1	Kawa	Temple A	Middle Napatan Period	Turquoise	Ring-shaped bead
MAN9341.2	Kawa	Temple A	Middle Napatan Period	Turquoise	Ring-shaped bead
MAN9335(a-d).1	Kawa	Kawa	Middle Napatan Period	Turquoise	Lotus flower inlay
MAN9335(d).1	Kawa	Kawa	Middle Napatan Period	Turquoise	Lotus flower inlay
MAN6498.1	Sanam	Cemetery	Middle Napatan Period	Pale turquoise	Ring-shaped bead
MAN6498.2	Sanam	Cemetery	Middle Napatan Period	Pale turquoise	Ring-shaped bead
MAN6513.1	Sanam	Cemetery, N1/727D	Middle Napatan Period	Pale faded turquoise	Melon-shaped bead
MAN6536-5.1	Sanam	Cemetery, N1/1181R/P	Middle Napatan Period	Turquoise	Ring-shaped bead
MAN6536-5.2	Sanam	Cemetery, N1/1181R/P	Middle Napatan Period	Turquoise	Ring-shaped bead
MAN5604.4	Faras	Cemetery 1, Grave 2072	Meroitic Period	Pale turquoise	Ring-shaped bead
MAN5604.5	Faras	Cemetery 1, Grave 2072	Meroitic Period	Pale grey	Ring-shaped bead
MAN5608(a).1	Faras	Cemetery 1, Grave 693	Meroitic Period (1st-2nd century CE)	Turquoise	Ring-shaped bead
MAN5608(b).2	Faras	Cemetery 1, Grave 693	Meroitic Period (1st-2nd century CE)	Turquoise	Ring-shaped bead
OE.8013.1	Meroe	Meroe	Meroitic Period	Light/pale Turquoise	Barrel-shaped bead
OE.8013.2	Meroe	Meroe	Meroitic Period	Turquoise	Cylindrical bead
OE.8063.1	Meroe	Meroe	Meroitic Period	Pale green	Cylindrical bead
OE.8063.2	Meroe	Meroe	Meroitic Period	Worn/green?	Cylindrical bead
OE.8063.3	Meroe	Meroe	Meroitic Period	Red/brown	Cylindrical bead
OE.8070.1	Meroe	Meroe	Meroitic Period	Pale green	Large Round bead

New Kingdom c.1450BC.

The six samples from the Garstang Museum all date to the Meroitic Period and came from the royal capital at Meroe excavated by Garstang but are only listed as coming broadly from 'Meroe'. (See Török, 1997 for problems associated with provenances and contexts for material from Garstang's excavations.)

These 30 samples were mounted in resin, ground to 1200 µm, polished to a 1 µm finish, and then given a 20 nm layer of carbon (see Newbury and Ritchie, 2015 for best practices). Analysis was performed on a JEOL JSM-IT300 Scanning Electron Microscope (SEM) equipped with a Bruker XFlash6-30 Energy Dispersive Spectrometer (EDS) detector in the Professor Elizabeth Slater Archaeology Laboratories at the University of Liverpool. Primary calibration was done by collecting spectra from a multi-element MAC block before using Corning A, B, and C polished to 0.25 µm and given a 20 nm coating of carbon as the standard reference materials (SRM). This established the error and reproducibility of the EDS data compared with internationally known certified values (see Table 4 for results of SRM compared to accepted values detailed by Adlington, 2017).

The elements of interest were silicon (Si), calcium (Ca), sodium (Na), potassium (K), magnesium (Mg), manganese (Mn), copper (Cu), cobalt (Co), lead (Pb), iron (Fe), aluminium (Al), antimony (Sb), and titanium (Ti), and will be expressed here as oxides.

The SRMs and samples were analysed using the same parameters; 20 kV accelerating voltage, 50nA probe current, and a working distance (WD) of 10 mm, for 60 s. For the sample analysis, the areas visually identified—using the backscatter electron images (BEI)—as the glaze

layer, the interaction layer, and the body, were analysed three times and an average taken. In some cases, due to the physical condition of some of the samples examined here due to weathering (either pre- or post-excavation), it was not always possible to identify whether there were remaining glaze and interaction layers to analyse.

3. Results (chemical and visual analysis)

The visual and chemical analyses presented a mixed set of results due to the physical condition of the faience examined. This may be connected with both the original production quality and potential decay following deposition (see Hench and Clark, 1978; Munier et al., 2002; Dal Bianco et al., 2005; Tournié et al., 2008; Vilarigues and da Silva, 2009; Gentaz et al., 2012; Won-In et al., 2012; van Elteren et al., 2013; Panighello et al., 2015, for discussions of vitreous decay with reference to glass and the environments in which it can occur). The normalised results of the chemical analysis are presented in Tables 5–9.

Due to the potentially weathered nature of 16 of the faience samples, those with total analysed values of their glaze layer, interaction layer, and/or body that were not within 97–103 wt% also have their non-normalised values presented in Appendix Table A1. This was done in order to be able to identify any elements present that might indicate decay and to highlight the values of particular components that were lower than would be expected. It is still possible, however, to suggest a glazing technique based on the levels of the identified colourant. Despite their apparently decayed state, some of the Meroitic Period material had begun to deteriorate to such an extent that it fell apart.

Table 4

Mean values, standard deviation, %error, and %precision for the Corning Standards A, B, and C and from Adlington (2017).

Corning A													
Oxides	Na ₂ O	MgO	Al ₂ O ₃	SiO ₂	K ₂ O	CaO	TiO ₂	MnO	Fe ₂ O ₃	CoO	CuO	Sb ₂ O ₅	PbO
Average (6) (wt%)	14.49	3.80	0.63	68.08	3.07	5.42	1.14	1.08	1.11	0.09	1.12	2.01	0.12
Accepted (wt%)	14.30	2.66	1.00	66.56	2.87	5.03	0.79	1.00	1.09	0.17	1.17	1.75	0.07
SD	0.10	0.57	0.19	0.76	0.10	0.19	0.18	0.04	0.01	0.04	0.03	0.25	0.03
%Error (±)	1.34	43.02	37.29	2.29	6.92	7.67	44.67	8.00	1.44	45.38	4.27	28.00	7.55
%Precision (±)	14.73	28.58	33.27	4.93	17.02	15.89	18.15	18.72	23.53	38.49	18.10	12.95	137.48
CORNING B													
Oxides	Na ₂ O	MgO	Al ₂ O ₃	SiO ₂	K ₂ O	CaO	TiO ₂	MnO	Fe ₂ O ₃	CoO	CuO	Sb ₂ O ₅	PbO
Average (6) (wt%)	18.10	0.94	3.96	63.85	1.14	9.31	0.06	0.25	0.30	0.01	2.54	0.16	0.61
Accepted (wt%)	17.00	1.03	4.36	61.55	1.00	8.56	0.08	0.25	0.34	0.04	2.66	0.46	0.61
SD	0.55	0.05	0.20	1.15	0.07	0.38	0.01	0.00	0.02	0.02	0.06	0.15	0.00
%Error (±)	6.49	8.74	9.24	3.74	14.14	8.80	19.64	1.71	12.61	82.14	4.62	65.22	0.23
%Precision (±)	10.39	46.17	16.04	4.37	24.37	14.96	69.99	31.87	25.10	162.48	13.86	101.05	94.17
CORNING C													
Oxides	Na ₂ O	MgO	Al ₂ O ₃	SiO ₂	K ₂ O	CaO	TiO ₂	MnO	Fe ₂ O ₃	CoO	CuO	Sb ₂ O ₅	BaO
Average (4) (wt%)	ND	1.90	ND	36.22	2.49	4.67	1.65	ND	0.11	0.07	0.97	ND	39.165
Accepted (wt%)	1.07	2.76	0.87	34.87	2.84	5.07	0.79	0.0011	0.34	0.18	1.13	—	36.7
SD	0.54	0.43	—	0.68	0.18	0.2	0.43	—	0.11	0.06	0.08	—	1.23
%Error (±)	100.00	30.98	—	3.89	12.32	7.89	109.49	—	66.18	61.11	14.16	—	6.72
%Precision (±)	—	46.98	—	3.05	7.63	10.49	25.68	—	21.74	100.00	12.37	—	5.63

Table 5

Normalised results in wt% for C-Group Phase Ia (ND indicates not detected when a value of 0.00 wt% was given).

C-GROUP PHASE IA													
Faiience component	Na ₂ O	MgO	Al ₂ O ₃	SiO ₂	K ₂ O	CaO	TiO ₂	MnO	Fe ₂ O ₃	CoO	CuO	Sb ₂ O ₅	PbO
MAN8439a.1													
Glaze layer	ND	ND	ND	97.80	0.03	0.18	0.04	0.04	0.26	ND	1.52	0.13	ND
Interaction layer	0.04	ND	ND	98.29	0.07	0.74	0.07	0.02	0.17	0.01	0.44	0.13	ND
Body	ND	0.08	0.06	97.78	0.03	1.24	0.07	0.02	0.20	ND	0.40	0.08	0.02
MAN8439a.2													
Glaze layer	ND	ND	ND	97.29	0.11	0.76	ND	0.01	0.31	0.05	1.20	0.15	0.11
Interaction layer	0.30	0.02	ND	98.49	0.04	0.16	0.06	ND	0.16	ND	0.51	0.10	0.14
Body	0.09	0.07	ND	98.84	0.06	0.215	0.03	ND	0.19	0.01	0.18	0.05	0.24

Table 6

Normalised results in wt% for Classic Kerma Period samples (ND indicates not detected when a value of 0.00 wt% was given).

Classic Kerma Period													
MAN8561.1													
Faience component	Na ₂ O	MgO	Al ₂ O ₃	SiO ₂	K ₂ O	CaO	TiO ₂	MnO	Fe ₂ O ₃	CoO	CuO	Sb ₂ O ₅	PbO
Outer body	2.85	ND	ND	80.55	0.31	1.06	ND	0.01	0.17	0.11	14.76	0.05	0.11
Inner body	10.14	0.09	0.88	79.17	3.12	1.63	0.16	0.08	0.85	0.03	3.72	0.03	0.06
MAN8561.2													
	Na ₂ O	MgO	Al ₂ O ₃	SiO ₂	K ₂ O	CaO	TiO ₂	MnO	Fe ₂ O ₃	CoO	CuO	Sb ₂ O ₅	PbO
Outer body	10.68	ND	ND	69.99	4.96	4.74	0.03	0.02	0.15	ND	9.40	ND	ND
Inner body	0.89	ND	0.20	94.26	0.58	0.43	ND	0.03	0.25	ND	3.07	ND	0.28
MAN8561.3													
	Na ₂ O	MgO	Al ₂ O ₃	SiO ₂	K ₂ O	CaO	TiO ₂	MnO	Fe ₂ O ₃	CoO	CuO	Sb ₂ O ₅	PbO
Outer body	3.13	0.03	0.05	79.56	0.44	0.32	0.03	0.04	0.12	ND	15.66	0.11	0.50
Inner body	10.69	0.2	0.65	79.28	3.41	0.55	0.08	0.02	0.76	ND	4.25	0.01	0.07
MAN8561.4													
	Na ₂ O	MgO	Al ₂ O ₃	SiO ₂	K ₂ O	CaO	TiO ₂	MnO	Fe ₂ O ₃	CoO	CuO	Sb ₂ O ₅	PbO
Outer body	2.27	0.07	ND	82.44	1.70	3.95	0.05	ND	0.04	0.01	9.44	0.02	ND
Inner body	0.20	ND	ND	96.22	0.40	0.21	0.09	0.05	0.28	0.01	2.33	0.09	0.09
MAN8561.5													
	Na ₂ O	MgO	Al ₂ O ₃	SiO ₂	K ₂ O	CaO	TiO ₂	MnO	Fe ₂ O ₃	CoO	CuO	Sb ₂ O ₅	PbO
Outer body	10.57	0.17	0.05	70.96	4.47	4.22	0.03	0.04	0.14	ND	9.23	0.10	ND
Inner body	1.06	ND	0.03	94.16	0.89	0.35	0.07	0.04	0.39	0.07	2.87	0.04	ND
MAN8561.6													
	Na ₂ O	MgO	Al ₂ O ₃	SiO ₂	K ₂ O	CaO	TiO ₂	MnO	Fe ₂ O ₃	CoO	CuO	Sb ₂ O ₅	PbO
Outer body	2.78	0.02	0.05	78.37	1.06	1.61	0.06	0.06	0.35	0.01	15.13	0.10	0.37
Inner body	12.09	0.29	0.20	78.10	3.34	1.26	0.03	0.01	0.55	0.02	4.09	ND	ND

Table 7

Normalised results in wt% for New Kingdom samples (ND indicates not detected when a value of 0.00 wt% was given).

New Kingdom													
MAN8442a-e.3													
Faience component	Na ₂ O	MgO	Al ₂ O ₃	SiO ₂	K ₂ O	CaO	TiO ₂	MnO	Fe ₂ O ₃	CoO	CuO	Sb ₂ O ₅	PbO
Glaze layer	0.25	0.19	0.12	95.72	0.10	1.09	0.02	0.01	0.37	0.06	1.89	ND	0.16
Body	0.19	0.28	ND	97.85	0.06	0.52	0.02	0.02	0.57	0.08	0.41	ND	ND
MAN8442a-e..4													
	Na ₂ O	MgO	Al ₂ O ₃	SiO ₂	K ₂ O	CaO	TiO ₂	MnO	Fe ₂ O ₃	CoO	CuO	Sb ₂ O ₅	PbO
Body	0.17	0.15	ND	98.76	0.10	0.26	ND	ND	0.30	ND	ND	ND	0.27
MAN8442a-e.5													
	Na ₂ O	MgO	Al ₂ O ₃	SiO ₂	K ₂ O	CaO	TiO ₂	MnO	Fe ₂ O ₃	CoO	CuO	Sb ₂ O ₅	PbO
Body	ND	ND	ND	98.57	0.07	0.13	0.23	0.03	0.43	ND	0.08	ND	0.48

The results presented below (Tables 5–9) will be discussed by time period so as to inform about chemical composition and the glazing technique, as well as to permit any changes/similarities to be observed over the time periods examined here.

3.1. C-group phase Ia (c.2160–2055BC)

The two samples from this time period show that their glaze, interaction layer, and body are predominantly composed of SiO₂ with the 1.52 wt% and 1.20 wt% CuO (MAN8439a.1 and MAN8439a.2 respectively) providing their pale green/blue colour. Of interest with these samples is the comparatively low levels of Na₂O present throughout, and the 1.25 wt% value of CaO in the body of MAN8439a.1. The values for CuO reduce immediately in both the interaction layer and the body that suggests the glazing method of cementation. There is no clear interparticle glass present in the body (see Fig. 2). The presence of interparticle glass is normally associated with efflorescence glazing (see Tite and Shortland, 2008) although experimental archaeology has shown its potential to be present when the cementation glazing method is used (Matin and Matin, 2012; 2016). In this case, however, as the interparticle glass appears to be absent, then it could be considered that cementation glazing was used on these samples.

3.2. Classic Kerma Period (c.1700–1550BC)

Within the dataset examined here, the Classic Kerma Period samples are the most homogenous and due to this no glaze, interaction, or body layer could be established for analysis and therefore analyses were taken on the outer body—here referring to the part of the sample closest to the surface—and the inner body—referring to analyses taken from the inside of the sample. In all cases they have very high levels of CuO, which explains their dark blue colour, and unlike the C-Group Phase Ia samples they are the same colour all the way through. Two samples MAN 8561.1 and MAN8561.5 show the presence of CoO, however due to the limits of detection of SEM-EDS, additional analyses using a method with a higher limit of detection for CoO would be needed. The samples' SiO₂ levels are generally lower than those from the C-Group Phase Ia whilst the Na₂O levels are noticeably higher as are the K₂O levels, which may indicate the use of a mixed alkali for these specific samples. The Na₂O levels of MAN8561.2 and MAN8561.5 show a higher soda level in the outer body than the inner body which is in contrast to the other samples. It is when these samples are examined visually that an interesting observation can be made. Fig. 3 shows the six samples using BEI. Unlike those of the C-Group Phase Ia samples (see Fig. 2 above) there is no clear sign of what could be recognised as a glaze layer. This, combined with the chemical results, introduces for the first time the possibility of an identification of the presence of glassy faience—also known as Variant E—at the site of Kerma and this will be discussed below. The term 'Variant E' comes from

Table 8

Normalised results in wt% for Middle Napatan Period samples (ND indicates not detected when a value of 0.00 wt% was given). Non-normalised results for samples suffering from decay are included in Appendix Table A7.

Middle Napatan Period													
MAN9341.1													
Faiience component	Na ₂ O	MgO	Al ₂ O ₃	SiO ₂	K ₂ O	CaO	TiO ₂	MnO	Fe ₂ O ₃	CoO	CuO	Sb ₂ O ₅	PbO
Glaze layer	0.60	0.11	ND	88.33	0.02	4.97	0.08	0.06	0.23	0.02	5.49	0.04	0.09
Body	ND	ND	0.14	97.28	0.05	0.45	0.04	ND	0.71	ND	1.19	0.04	0.10
MAN9341.2													
Glaze layer	0.85	ND	ND	87.46	ND	3.34	0.02	0.10	0.07	0.02	8.15	ND	ND
Body	ND	ND	0.13	97.47	0.23	0.32	0.03	0.07	0.80	0.02	0.78	0.14	ND
MAN9335.1													
Glaze layer	0.39	ND	0.65	89.44	0.41	0.95	0.06	ND	0.49	0.05	6.54	0.49	0.51
Body	0.07	ND	0.35	96.79	0.22	0.24	0.01	0.01	0.20	ND	1.48	0.07	0.53
MAN6498.1													
Glaze layer	0.56	ND	1.43	95.79	0.10	0.17	0.08	ND	0.13	0.01	1.43	0.03	0.25
Interaction layer	ND	ND	0.77	97.23	0.29	0.17	0.02	ND	0.37	0.03	1.11	ND	ND
Body	0.39	ND	1.21	95.71	0.39	0.26	0.06	0.02	0.83	0.11	0.86	0.12	0.01
MAN6498.2													
Glaze layer	1.69	ND	2.62	89.91	0.49	0.21	0.17	0.06	2.05	0.04	2.48	0.25	ND
Interaction layer	2.47	ND	1.63	91.4	0.96	0.34	0.08	0.01	0.93	ND	1.28	0.38	0.51
Body	2.08	ND	2.12	90.65	0.72	0.27	0.12	0.03	1.49	0.02	1.88	0.31	0.25
MAN6513.1													
Glaze layer	0.14	ND	0.67	72.71	0.01	0.62	0.23	0.02	2.98	ND	1.39	0.07	21.15
Interaction layer	3.58	ND	1.59	82.71	1.52	0.15	0.02	0.02	3.51	0.05	0.13	0.47	6.24
Body	0.53	ND	0.32	91.75	0.40	0.26	0.06	0.11	1.585	ND	0.01	0.38	4.58
MAN6536-5.1													
Glaze layer	0.86	ND	1.04	83.36	0.16	1.95	0.01	0.04	0.48	0.02	11.87	0.07	0.12
Interaction layer	1.05	ND	1.89	91.17	0.44	0.83	0.03	0.14	0.41	0.04	3.80	0.20	ND
Body	6.38	0.19	0.74	85.79	1.73	0.41	0.11	0.18	0.68	0.02	3.45	0.22	0.07
MAN6536-5.2													
Glaze layer	0.53	ND	0.70	82.96	0.07	2.34	0.04	0.08	0.55	0.01	11.90	0.11	0.67
Interaction layer	ND	ND	0.98	92.1	0.25	0.73	0.04	0.04	0.88	ND	4.54	0.03	0.41
Body	0.30	ND	1.00	93.46	0.24	0.64	0.05	0.03	0.42	0.01	3.69	0.13	ND
MAN9335(d).1													
Glaze layer	0.04	ND	0.16	98.50	0.09	0.44	0.01	ND	0.06	ND	0.52	ND	0.16
Body	0.13	0.13	0.13	97.16	0.12	1.57	0.02	0.01	0.46	0.10	0.14	ND	0.01

Lucas (Lucas and Harris, 1962). Kaczmarczyk and Hedges (1983), as part of their re-evaluation of Lucas' variant system, considered 'glassy faience' a misnomer and as there was no distinct outer layer, the term faience was inappropriate and made the suggestion of the alternative name of 'imperfect glass' (Kaczmarczyk and Hedges, 1983: 212). Variant E and glassy faience as terms have still been used in publications since (e.g. Tite and Shortland 2008). Whilst it is recognised that glassy faience as a term does have difficulties, imperfect glass perhaps indicates that the resulting product was intended as a glass. While such a term could be appropriately used when glass was being produced as a separate man-made raw material, at a time period when there is no evidence of the deliberate production of glass—and given the macroscopic similarities between faience and glassy faience—then it is perhaps not correct to use this term here. The term glassy faience does reflect that this material is not quite a proper glass but neither is it a proper faience, falling somewhere in-between. Therefore, the term Variant E is used here when citing other authors but the Classic Kerma Period samples discussed here will be referred to as 'glassy faience'.

3.3. New Kingdom (c.1550–1069BC)

Of the three samples dated to the New Kingdom examined here, which all comprise vessel fragments, only one had a discernible glaze layer for analysis. This sample (MAN8442a-e.3, Table 3) is a grey/green vessel fragment that showed 1.89 wt% CuO. The level of CuO noticeably

reduces in the body and this combined with little visual evidence of interparticle glass may indicate cementation glazing. Matin and Matin, 2012; 2016 have shown the potential for interparticle glass to also be present in cementation glazing but the condition of this sample makes it hard to confirm a glazing technique here. As the other samples do not have a glaze layer that could be analysed and CuO levels that were very low or below detection limits, it is not possible to tell whether this was the colourant or to confirm a glazing method. Fig. 4 highlights the state of this faience and shows that rather than the expected quartz grains held in a glassy matrix with a glazing layer and body (with a possible identifiable interaction layer between), this material is made of very large angular quartz grains held within a matrix of smaller quartz grains. This may be an indication of the use of crushed stone versus the use of sand which may show more rounded grains due to natural weathering processes.

3.4. Middle Napatan period (c.780–656BC)

The Napatan period samples are once more from beads and present a more varied set of results. This variability may in part be due to weathering. The levels of CuO present in these samples, whilst indicating its use as a possible colourant, are very varied. In terms of the glazing, there is the presence of CuO through the glaze and into the body (and the interaction layer when it could be identified microscopically), alongside interparticle glass (see Fig. 5). This could be an indication of

Table 9

Normalised results in wt% for Meroitic Period samples (ND indicates not detected when a value of 0.00 wt% was given). Non-normalised results for samples suffering from decay are included in Appendix Table A7.

Meroitic Period													
MAN5604.4													
Faience component	Na ₂ O	MgO	Al ₂ O ₃	SiO ₂	K ₂ O	CaO	TiO ₂	MnO	Fe ₂ O ₃	CoO	CuO	Sb ₂ O ₅	PbO
Glaze layer	0.01	ND	0.07	99.40	ND	0.06	0.03	0.02	0.03	ND	0.27	0.04	0.05
Body	0.09	ND	0.50	96.15	0.21	0.30	0.08	0.08	0.40	0.07	1.85	0.16	0.08
MAN5604.5													
	Na ₂ O	MgO	Al ₂ O ₃	SiO ₂	K ₂ O	CaO	TiO ₂	MnO	Fe ₂ O ₃	CoO	CuO	Sb ₂ O ₅	PbO
Glaze layer	2.23	15.33	11.58	48.68	0.94	6.63	0.62	0.06	6.71	0.02	7.02	0.10	0.06
Body	ND	ND	0.42	93.43	0.19	4.22	0.01	0.01	0.77	0.07	0.64	ND	0.22
MAN5608(a).1													
	Na ₂ O	MgO	Al ₂ O ₃	SiO ₂	K ₂ O	CaO	TiO ₂	MnO	Fe ₂ O ₃	CoO	CuO	Sb ₂ O ₅	PbO
Glaze layer	0.83	0.02	0.78	89.90	0.01	1.60	0.03	0.08	0.17	ND	5.07	ND	1.48
Interaction layer	0.72	ND	1.41	93.25	0.19	0.76	0.08	ND	0.73	0.03	1.76	0.13	0.94
Body	1.99	0.06	0.75	93.04	0.48	1.00	0.09	0.01	0.63	ND	1.22	0.07	0.65
MAN5608(a).2													
	Na ₂ O	MgO	Al ₂ O ₃	SiO ₂	K ₂ O	CaO	TiO ₂	MnO	Fe ₂ O ₃	CoO	CuO	Sb ₂ O ₅	PbO
Glaze layer	4.10	0.02	6.96	83.66	1.34	0.45	0.05	0.03	0.93	0.03	1.72	ND	0.67
Interaction layer	0.69	0.55	1.29	93.39	ND	0.67	0.02	ND	0.58	ND	1.87	ND	0.93
Body	1.49	ND	0.66	93.46	0.54	1.42	0.08	0.01	0.60	0.08	1.17	0.11	0.37
E.8013.1													
	Na ₂ O	MgO	Al ₂ O ₃	SiO ₂	K ₂ O	CaO	TiO ₂	MnO	Fe ₂ O ₃	CoO	CuO	Sb ₂ O ₅	PbO
Glaze layer	0.07	0.04	ND	97.28	0.05	1.06	0.01	ND	0.45	ND	0.70	ND	0.33
Body	0.24	0.15	0.04	96.84	0.16	1.39	0.02	ND	0.63	0.04	0.41	0.06	ND
E.8013.2													
	Na ₂ O	MgO	Al ₂ O ₃	SiO ₂	K ₂ O	CaO	TiO ₂	MnO	Fe ₂ O ₃	CoO	CuO	Sb ₂ O ₅	PbO
Glaze layer	1.13	1.52	0.51	86.43	0.31	1.34	0.01	0.01	0.42	0.11	7.67	0.12	0.38
Body	1.54	0.22	0.08	91.17	0.36	1.80	0.01	0.04	0.30	ND	2.73	1.68	0.58
E.8070.1													
	Na ₂ O	MgO	Al ₂ O ₃	SiO ₂	K ₂ O	CaO	TiO ₂	MnO	Fe ₂ O ₃	CoO	CuO	Sb ₂ O ₅	PbO
Glaze layer	0.17	0.09	0.01	97.98	0.24	0.88	0.02	0.01	0.19	ND	0.29	ND	0.09
Body	0.15	0.22	0.04	93.92	0.29	4.94	0.02	0.01	0.31	ND	0.06	ND	ND
E.8063.1													
	Na ₂ O	MgO	Al ₂ O ₃	SiO ₂	K ₂ O	CaO	TiO ₂	MnO	Fe ₂ O ₃	CoO	CuO	Sb ₂ O ₅	PbO
Glaze layer	ND	ND	0.79	95.86	0.67	0.28	0.03	0.04	0.34	0.05	1.83	0.09	ND
Body	0.11	0.06	0.34	97.71	0.43	0.36	0.07	ND	0.16	ND	0.72	ND	ND
E.8063.2													
	Na ₂ O	MgO	Al ₂ O ₃	SiO ₂	K ₂ O	CaO	TiO ₂	MnO	Fe ₂ O ₃	CoO	CuO	Sb ₂ O ₅	PbO
Glaze layer	ND	0.02	0.02	99.51	0.10	0.07	0.01	0.01	0.01	0.01	0.14	0.07	0.02
Body	ND	ND	0.03	96.27	0.28	0.27	0.01	0.01	0.67	0.02	1.81	0.23	0.39
E.8063.3													
	Na ₂ O	MgO	Al ₂ O ₃	SiO ₂	K ₂ O	CaO	TiO ₂	MnO	Fe ₂ O ₃	CoO	CuO	Sb ₂ O ₅	PbO
Glaze layer	ND	0.23	ND	98.44	0.19	0.41	0.01	0.01	0.53	0.02	0.05	0.08	ND
Body	0.13	ND	0.59	96.73	0.40	0.90	ND	0.06	0.58	0.06	0.16	0.01	0.34

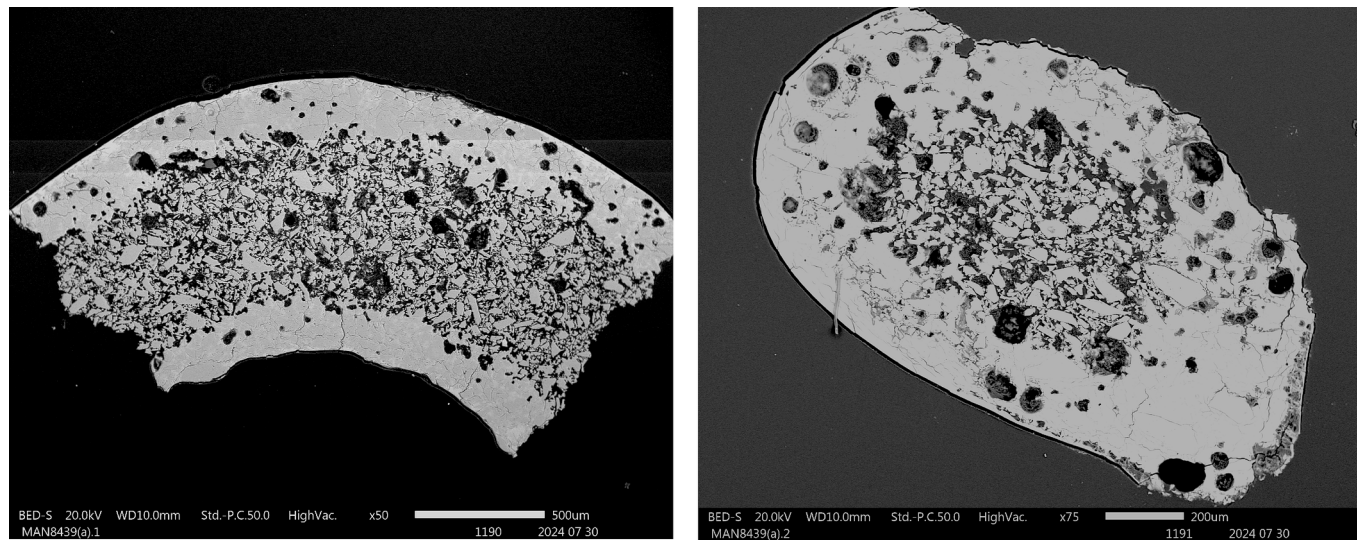


Fig. 2. BSE image of MAN8439(a.1) (left) and MAN8439(a.2) (right).

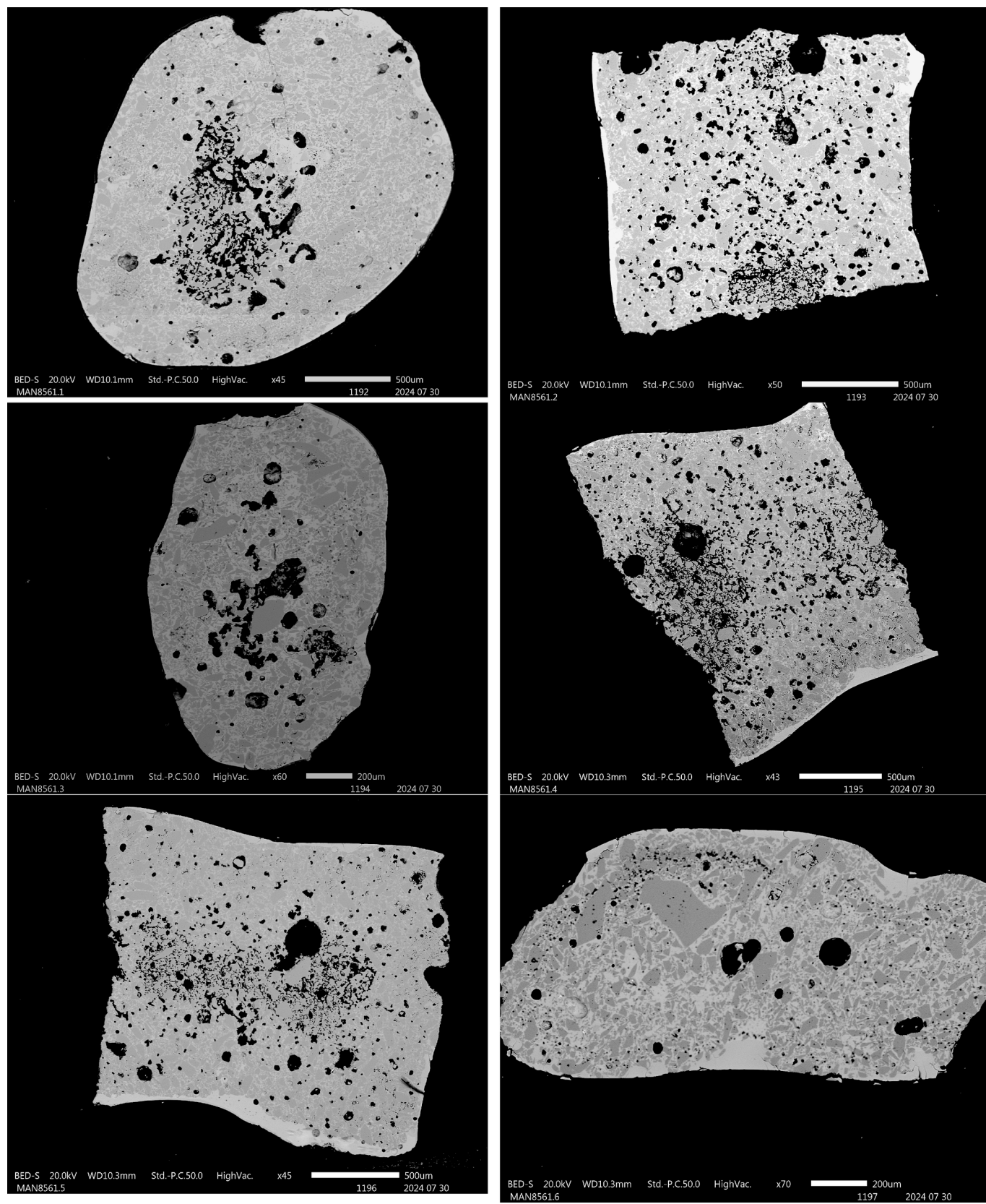


Fig. 3. BSE image of the Classic Kerma Period samples.

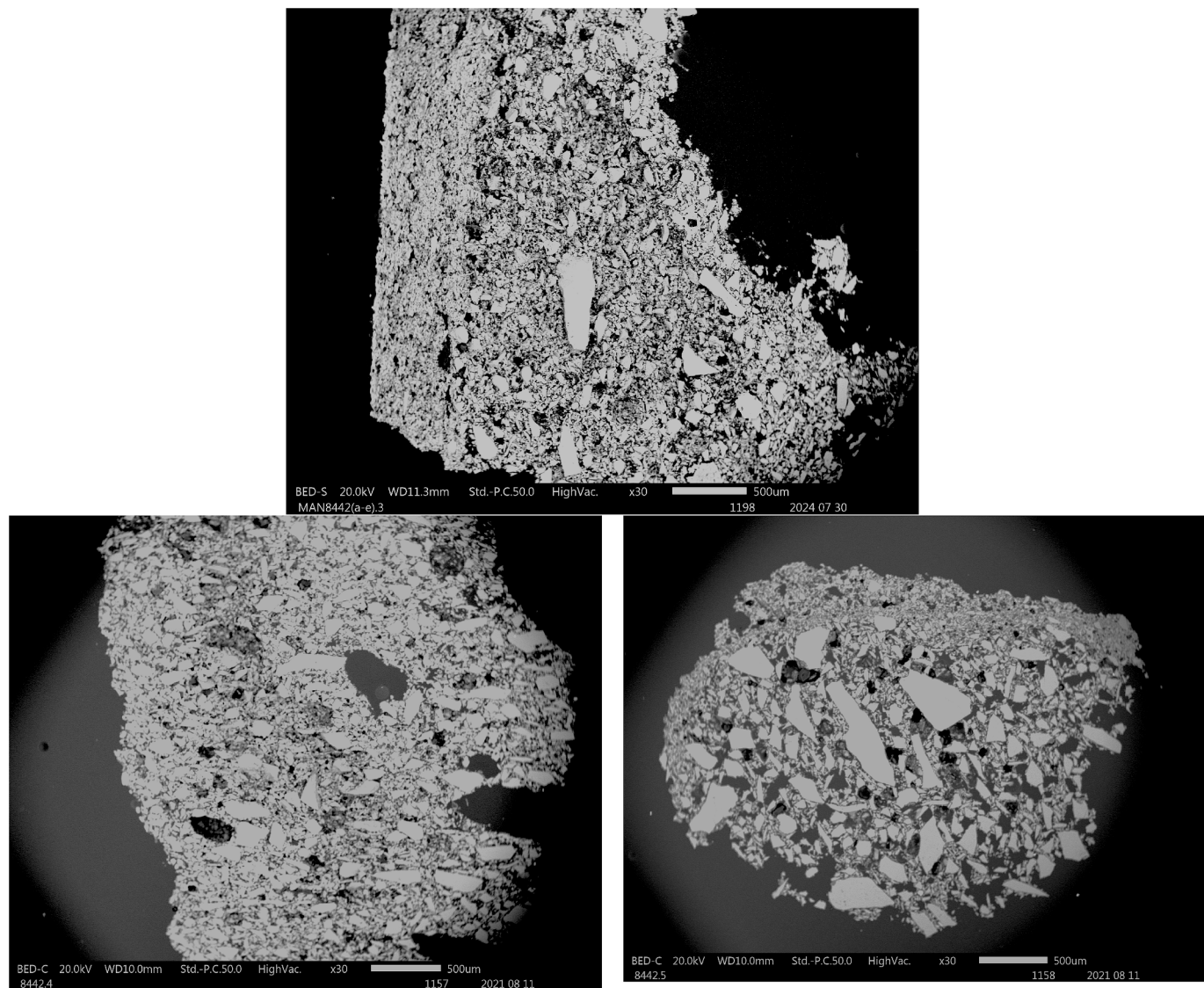


Fig. 4. BEI of MAN8442a-e.3 (top), MAN8442a-e.4 (bottom left), MAN8442a-e.5 (bottom right).

efflorescence glazing (see [Tite and Shortland, 2008](#)), however [Matin and Matin, 2012; 2016](#) have shown experimentally that interparticle glass can also be present as a result of cementation glazing therefore it is difficult to be certain here which method has been used. MAN9341.2, due to the noticeable drop in CuO levels, may have been glazed using the cementation method. In sample MAN6513.1, whilst the drop in and almost lack of CuO in the body and interaction layer of the sample could be an indication of cementation glazing this cannot be confirmed in light of the PbO levels. A number of the samples show very low Na₂O levels (below 1 wt%) whilst the CaO levels appear to show a marked difference between the glaze layer and the body. In two samples from the site of Kawa (MAN9341.1 and MAN9341.2), CaO levels decrease into the body, and this is also seen in samples MAN6536-5.1 and MAN6536-5.2 that were recovered from the site of Sanam.

Of particular interest is MAN6513.1, a bead from Sanam, which shows very high levels of PbO in the glaze layer (21.16 wt% in the glaze layer (normalised), 15.96 wt% (non-normalised)), which drops to around 6 wt% in the interaction layer before dropping further to around 4 wt% in the body. Additionally, in [Fig. 5](#), the bright white particles that can be seen are a visual indication of the presence of Pb (see [Tite and Shortland, 2008](#)). Unfortunately, only one sample from the corpus studied here shows this. These levels of PbO may indicate the use of a

PbO flux and this, in the context of other vitreous materials using lead, will be discussed below.

3.5. Meroitic period (350BC–AD350)

The Meroitic Period bead samples are, as with the Napatan ones, rather varied across the corpus examined here. Of interest is sample MAN5604.5 with MgO levels in its glaze layer (which is considered a true glass) of 15.34 wt% (12.53 wt% non-normalised), which is far higher than would be expected, although in glass such levels are an indication of decay, as might be the case with the lower levels of SiO₂ detected in the glaze layer and the body. Additionally, the Al₂O₃ levels are around 10 wt% and Fe₂O₃ above 5 wt%, which is higher than might be expected for faience. While the combination of these two compounds can be an indication of a different geographical source for the sand used than from Egypt, Nubia, or the Mediterranean (see for example [Tite and Shortland, 2008](#); [Schibille 2011](#); [Rosenow and Rehren, 2014](#); [Rehren et al., 2015](#); [Spedding 2023b](#)), here, given the readily availability of sand, then it is more probable that it is due to weathering or burial environment.

Sample MAN5608(a).1 shows above 1 wt% of PbO in the glaze, in [Fig. 6](#) there are also bright white Pb flecks. Whilst these levels of PbO are

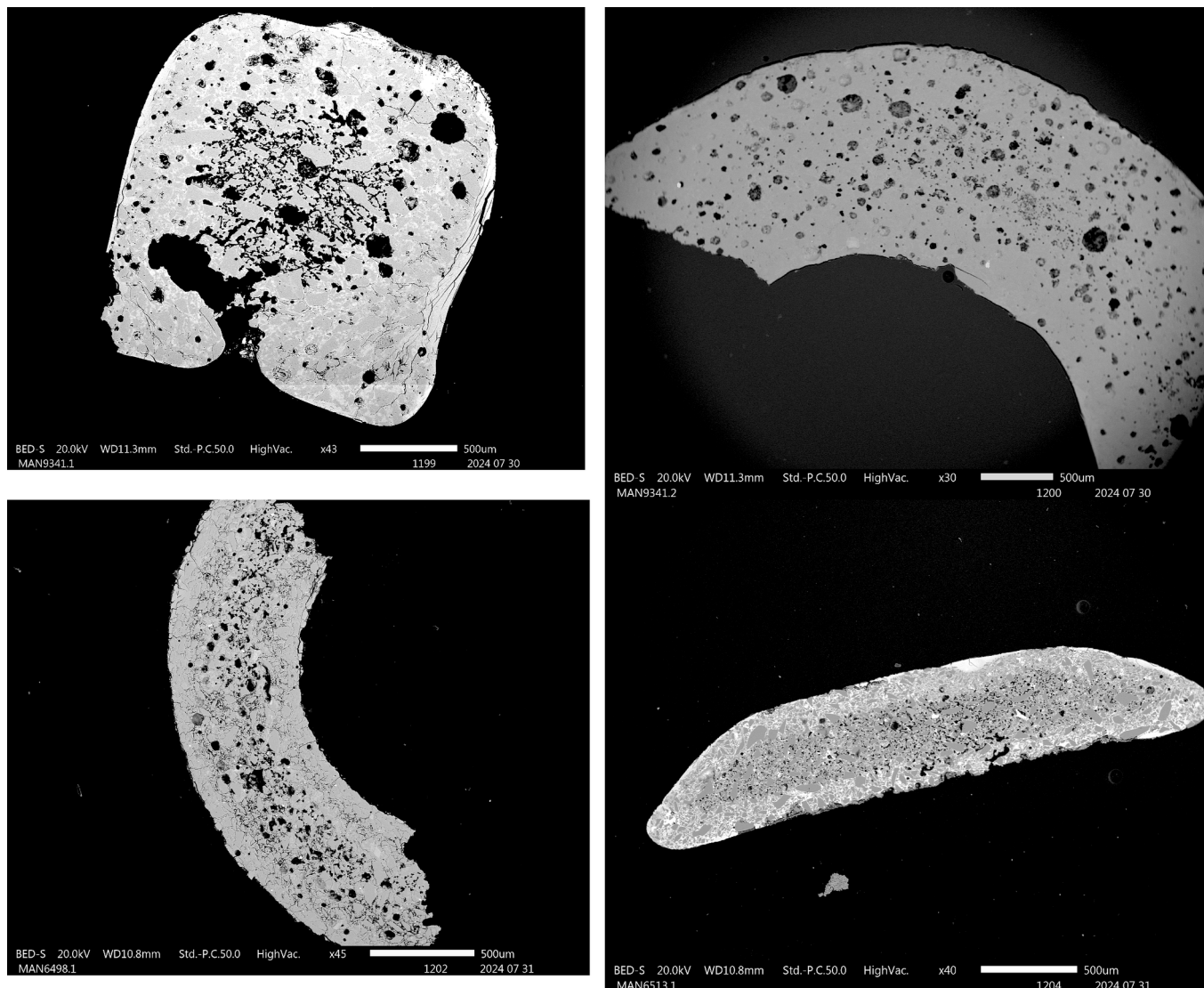


Fig. 5. BEI of example of Napatan samples and MAN 6513.1 (bottom right).

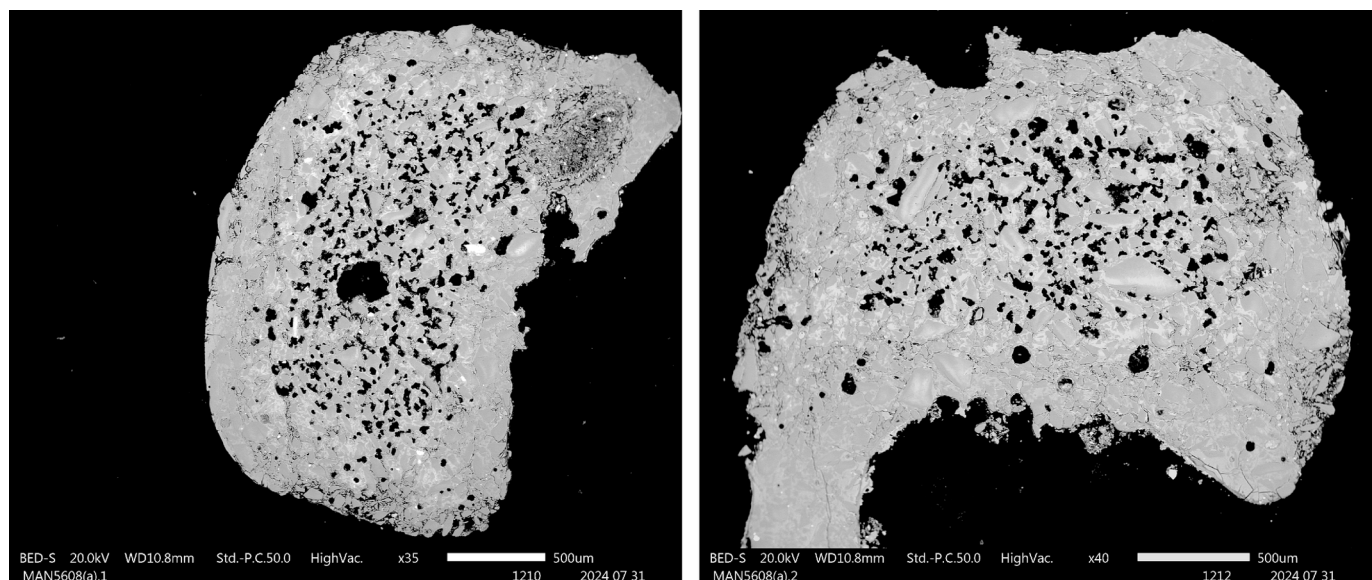


Fig. 6. BEI of MAN5608(a).1 (left) and MAN5608(a).2 (right).

Table 10

Average values for wt% of Variant E, Kerma, and Qasr Ibrim material. (Data from [Lucas and Harris, 1962](#); [Tite and Shortland 2008](#); [Spedding 2023a; 2023b](#)).

Sample	Context	SiO ₂	Na ₂ O	CaO	K ₂ O	MgO	Al ₂ O ₃	Fe ₂ O ₃	MnO
Variant E (Lucas and Harris)	?	88.60	5.80	2.10	0.30	—	1.40	0.40	—
Variant E (Tite and Shortland)	?	80.37	9.06	6.52	0.32	0.49	0.84	0.61 (FeO)	—
Qasr Ibrim (Spedding)	West Plaza, Central Stations, Level 9	84.29	8.75	0.47	0.75	0.12	0.71	0.58	0.04
Classic Kerma	Tumulus KX	81.92	5.62	1.70	2.06	0.07	0.18	0.34	0.04

not as high as was found in Napatan Period sample MAN6513.1, MAN5608(a).1 does stand out amongst the other Meroitic Period samples. Both MAN5608(a).1 and MAN5608(a).2 show, in Fig. 6, evidence of interparticle glass. [Matin and Matin \(2012; 2016\)](#) have shown its presence, experimentally, in cementation glazing. When this observation is combined with the CuO levels present throughout these samples there could be a potential case for the use of efflorescence glazing over cementation but this cannot be confirmed. The low levels of CuO detected in the body of E.8070.1 may indicate the use of cementation glazing for this sample.

4. Discussion

4.1. C-group phase Ia (c.2160–2055BC)

These samples are the oldest faience samples examined here.

Microscopic examination of the two bead samples revealed both had a very thick glaze layer (c.250–300 µm at its thickest) with a partially fused core (see Fig. 2). Voids are also clearly visible throughout. The very low levels of Na₂O detected (see Table 5) are also of interest. The CuO levels in the glaze identify it as the colourant with its levels dropping in the interaction layer and the body. This, combined with no clearly visible interparticle glass, presents a possible identification of cementation as the glazing technique (see [Tite and Shortland 2008](#)), although interparticle glass has been shown to have the potential to be present in cementation glazing ([Matin and Matin, 2012; 2016](#)). This allows for the consideration of the independent development of faience technology in Nubia alongside faience production in Egypt. Concerning Egyptian faience, [Nicholson et al. \(2009\)](#) suggest that cementation glazing does not appear until the Middle Kingdom (after C-Group Phase Ia, which is equivalent to the First Intermediate Period in Egypt, see Table 1). [Tite and Shortland \(2008\)](#) state that it is probable that all three

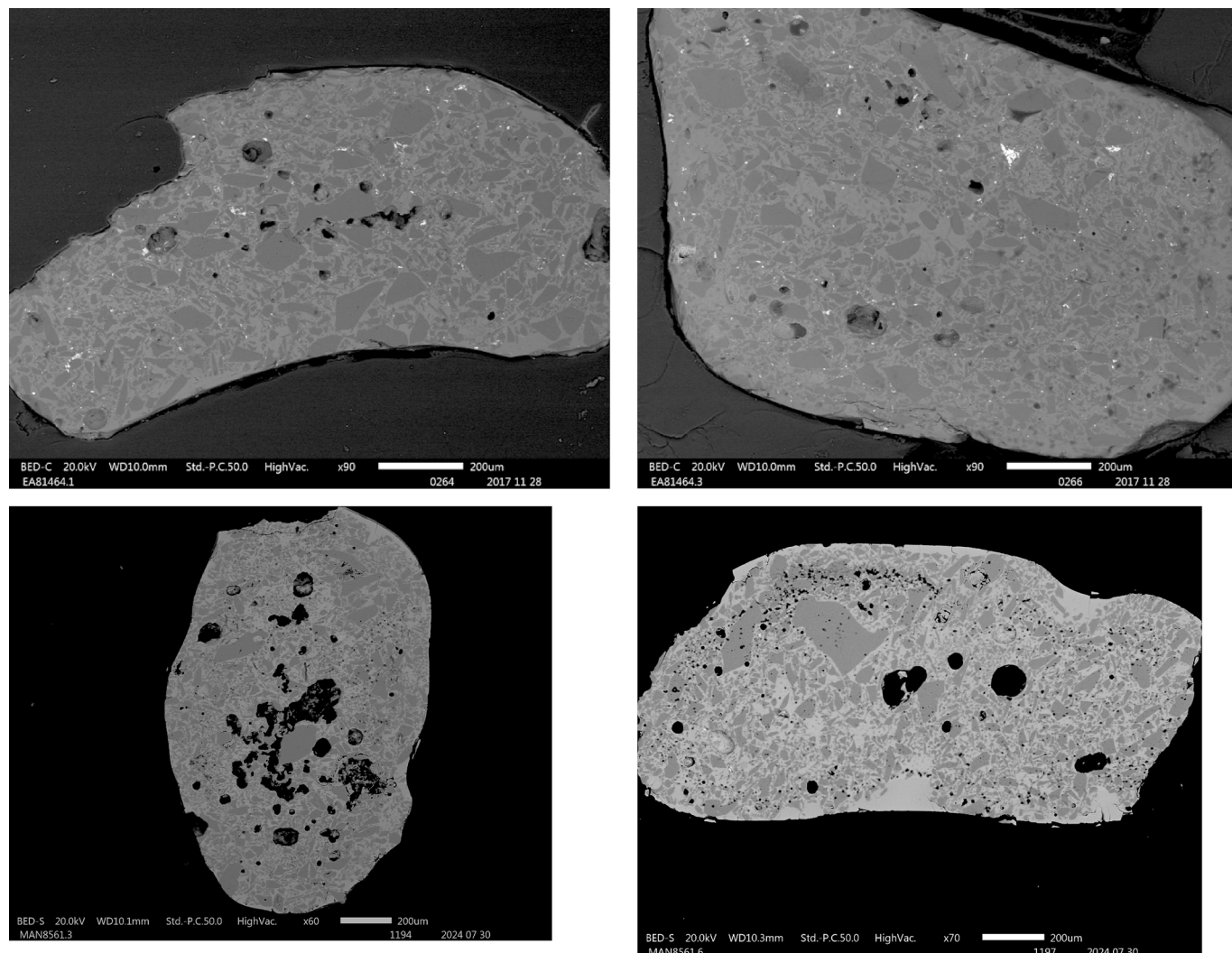


Fig. 7. Comparison of known glassy faience from the site of Qasr Ibrim ([Spedding 2023a; 2023b](#)) (top) to material from Kerma (bottom).

methods of glazing were used in the Predynastic Period (c.5300–3000BC), but that for the Egyptian Old Kingdom and First Intermediate Period (c.2686–2055BC) efflorescence glazing was ‘still probably dominant’ with cementation glazing being ‘more rarely’ used in the Middle Kingdom and Second Intermediate Period (c.2055–1550BC). Whilst these results only represent two samples and therefore no comment can be given on how extensively this method was used, it does show that cementation glazing technology was present in material from Lower Nubia and highlights a potential technological innovation and direction for faience production in Nubia. Such innovation could indicate an independence of the production and development of this material within the Nubian context. There is also the question about how widespread it may have been which would require additional provenanced samples to be analysed.

4.2. Classic Kerma Period (c.1700–1550BC)

The Classic Kerma Period dataset, due to their SiO₂ levels and appearance, presents the possibility of these samples being glassy faience. First identified by Lucas—his ‘Variant E’—early evidence for glassy faience may date to a 3rd Dynasty example from Djoser’s Step Pyramid complex, although the majority of examples would appear to date from the 25th/26th Dynasty (Lucas and Harris, 1962; Tite and Shortland 2008). Kaczmarczyk and Hedges (1983: 213) suggest its appearance in the 25th Dynasty and Late Period but cannot be sure ‘due to too few examples’. Table 10 presents the chemical values of the Classic Kerma Period samples, Variant E glassy faience (Lucas and Harris, 1962), samples dating to the 25th–26th Dynasties (Tite and Shortland 2008), and those identified from the Lower Nubian site of Qasr Ibrim dated to the Early Nobadia Period (c.350–600AD) by Spedding (2023a; 2023b).

Comparison of the average wt% of the SiO₂ and Na₂O with all six Classic Kerma samples does show a chemical similarity with the other samples in Table 10 but it is closer to the material from Lucas and Harris (1962) and Tite and Shortland (2008). A visual examination between the Classic Kerma samples and the glassy faience from Qasr Ibrim (see Fig. 7) also shows a visual similarity. Note that whilst glassy faience refers to a material that is not quite a glass and is also not quite faience, deliberately manufactured glass is not attested till around c.1500BC and microscopically would, ideally, not show any features, unlike faience or glassy faience (Shortland and Eremin, 2006).

Also present in the Classic Kerma samples is a higher level of K₂O (plant ash) which may be an indication of a different (mixed-alkali) flux for this material. This higher level of K₂O has also been observed in other faience produced at Kerma (see Lacovara, 2024), which Lacovara suggests was due to conflicts with Egypt resulting in access to faience and its raw materials (e.g. natron) being cut off and therefore the artisans at Kerma sought a different material in order to continue faience production (Lacovara, 2021; 2024). Other analytical examinations of faience tiles from the site of Kerma (see Lacovara, 2021; 2024) have shown a difference in the composition of the glaze and body of this material when compared to Egyptian faience further strengthening the case for local production, particularly seen in the imitation of Egyptian goods (e.g. basket weave vessels, a large hippopotamus figure, and a model boat similar to a gold example from the tomb of Ahhotep).

The presence of a locally produced glassy faience at Kerma could be considered to be part of the wider experimentation occurring at the site. Lacovara (2021; 2024) identifies local innovations of applying vitreous glazes to quartz crystal, milky quartz, and carnelian which continues traditions of glazed stone seen going back to the A-Group. All of this underscores the inventiveness and resourcefulness of the artisans at Kerma as they reinterpreted and utilised Egyptian material culture (Lacovara 2021; 2024). This production at Kerma would form the

foundation of locally-produced faience in Nubia during later periods (Lemos, 2024).

4.3. New Kingdom (c.1550–1069BC)

Unlike the C-Group Phase Ia and Kerma Period datasets, the New Kingdom samples were from three vessel fragments and came from a temple rather than a funerary context. This presented the opportunity to compare beads with vessel fragments. While macroscopically the objects these samples came from appear to be of acceptable quality, microscopic examination (see Fig. 4) reveals that they do not look like either faience or a glassy faience, thus raising questions about their production. This period in Nubia would see it under Egyptian colonial rule with recent work by Lemos (2024) highlighting that local faience production during this period builds upon the long history of faience production at Kerma, a long history shaped by both indigenous experiences and interactions with Egypt. In particular, an examination of faience shabtis from Aniba highlights the potential for innovation due to the unique decorative elements observed on them and whilst these have yet to be chemically investigated may still point to technical variability at the local level (Lemos, 2024). Smith and Buzon (2017) also discuss the influences and incorporations of Egyptian and Nubian practices and material goods in tombs at Tombos during the Egyptian New Kingdom that resulted in innovative and an ‘idiosyncratic interweaving of entangled cultural features’ (Smith and Buzon, 2017: 627).

4.4. Middle Napatan Period (c.780–656BC)

Returning to bead samples, the inclusion of these Napatan Period objects presented the opportunity to compare material from two different sites and contexts, with four samples from Kawa (two coming from a temple context (MAN9341.1, MAN9341.2) and two simply noted as being from the site itself (MAN9355(a-d).1, MAN9335(d).1). Of the five examples from Sanam, MAN6498.1, MAN6498.2 are noted as being from the cemetery, MAN6513.1 from N1/727D, and MAN6536-5.1 and MAN6536-5.2 from N1/1181R/P. The levels of CuO in both the glaze layer and body, as well as the presence of interparticle glass, indicates the use of efflorescence glazing in one of the Kawa samples (MAN9341.1). The CaO levels in this sample and in MAN9341.2 show a noticeable decrease between the glaze layer and the body. Similarly, the five Sanam samples also show evidence for efflorescence glazing due to the levels of CuO present in their body and glaze layers as well as the presence of interparticle glass.

Sample MAN6513.1 from Sanam is of particular interest here as it has high levels of PbO present in both its glaze layer and body material. Chemically, there are low levels of Na₂O detected in MAN6513.1 but—as is known from glass compositions—PbO can act as an alkali, which may explain not only the good condition of MAN6513.1 but also the lower levels of Na₂O (one of the more usual alkali sources) when compared to faience more generally. It was suggested that lead in glass helped it to resist weathering/decay (Freestone et al., 2003; Barber et al., 2009). This is borne out when comparing glasses with high amounts of lead to those with low amounts of lead from the same deposition environment based on glasses found at Faras and Gabati (Spedding, Forthcoming). What is of interest when examining the development of vitreous materials during the time of these Napatan Period objects, is the first appearance of high-lead red glass in Assyria, with this technologically demanding glass type also known to be present in Nubia in the Meroitic Period (Spedding 2018; 2022; 2023b). The level of PbO in MAN6513.1 drops noticeably between the glaze and interaction layers, although it is still higher in the interaction and body material than was found in any other sample analysed here. Material published by Tite and Shortland (2008) does not show any faience from Egypt of a

Table 11

Nubian faience production technology developments based on samples analysed here.

Date	Glazing method(s)	Attested	Object	Colours	Developments
C-Group Phase Ia	Cementation	Faras	Beads (ring-shaped)	Pale green/blue	Cementation glazing
Kerma Period	N/A	Kerma	Beads (ring-shaped)	Dark turquoise	Glassy faience
New Kingdom	Maybe cementation	Faras	Vessels	Green Grey Brown	Vessels Appearance of different colours
Napatan Period	Efflorescence Cementation	Kawa Sanam	Beads (ring-shaped, melon-shaped)	Turquoise	Appearance of high PbO content Efflorescence and cementation glazing
Meroitic Period	Efflorescence Cementation	Faras Meroe	Beads (ring-shaped, cylindrical)	Red Buff Turquoise Green	Efflorescence and cementation glazing Additional colours

similar time period with PbO present. Smith (2022) has highlighted the mutual influence of Nubia and Egypt on each other in the Iron Age and that Nubia was not a passive consumer but an active participant in the wider international world of the exchange of goods and ideas. Therefore, as could be seen in high-lead red glass found in Nubia during the Meroitic Period (Spedding 2023b), the presence of these high Pb levels in this faience object may be another example of the incorporation of potentially external ideas in the creation of faience in Nubia. Unfortunately, as only one sample shows these high levels of Pb it is not possible to suggest how widespread (or not) these levels might have been in faience from Nubia more generally or whether this is a site-specific phenomenon.

Analysis of Napatan Period faience has shown an irregular thickness of the glaze layer as well as a high copper content observed in many of the samples along with lower Na₂O and K₂O levels (see Lacovara, 2024). This is consistent with a number of the samples analysed here (MAN6536-5.1 and MAN6536-5.2 show CuO levels about 10 %, with MAN9341.2 at c.8 wt%). The Na₂O levels are, on average, lower for the samples analysed here than those in Lacovara (2024) with K₂O levels consistently low for the samples analysed here. These compositional levels along with the presence of high levels of PbO may be an indication of what Lacovara (2024, 52) considers to be a 'second reinvention of the process' of faience production which he suggests is, again, due to an interruption in trade with Egypt as a result of political hostilities.

4.5. Meroitic period (c.350BC–AD350)

The Meroitic Period bead samples are from a known cemetery context, with four of the samples coming from two graves at Faras (samples MAN5604.4, MAN5604.5, MAN5608(a).1, MAN5608(a).2) and the remaining six samples (E.8013.1, E.8013.2, E.8063.1, E.8063.2, E.8063.3, E.8070.1) coming from the site of Meroe. The combination of chemical and/or visual analysis permitted an identification of efflorescence (MAN5608(a).1, MAN5608(a).2, E.8013.2, E.8063.2) or cementation (MAN5604.5, E.8063.1, E.8070.1) glazing, while the glazing of a few of the samples remained unclear. It is worth noting that both glazing techniques are observed at each site.

Of interest, as with MAN6513.1 from the Napatan Period, sample MAN5608(a).1 from Faras has higher levels of PbO in its body and glaze layer than any of the other Meroitic samples analysed here. Visually this sample (see Fig. 6) shows a discernible glaze layer, fused vitreous material, and a few bright flecks that, as with MAN6513.1, could be a visual indication of Pb (see Tite and Shortland, 2008). MAN5604.5 has higher levels of Al₂O₃ and Fe₂O₃ than would normally be expected. Additionally, it has over 15 wt% of MgO. Advanced levels of MgO and Al₂O₃ have been observed in the corroded layer of African glasses in Panighello et al.'s study (2015). High levels of CuO have been observed in the Meroitic Period samples, over 7 wt% in MAN5604.5 and E.8013.2, and over 5 wt % in MAN5608(a).1. Of interest is the higher level of CuO observed in

the body of MAN5604.4 compared to its glaze layer (0.27 wt% in the glaze compared to 1.85 wt% in the body). This may be a further indication of decay, especially with the Na₂O levels being only 0.01 wt% and 0.09 wt% in the glaze and body respectively.

The Meroitic Period would see local faience production continue with recent analyses showing, once again, a glaze layer composition that was very different to contemporary faience produced in Egypt (see Lacovara, 2024).

5. Conclusion

The results above have allowed for the creation of a preliminary schema (Table 11) showing the development of faience from Nubia over the time periods covered by the material examined here. With further examinations of more faience from Nubia there will be the opportunity to amend Table 11 to get a fuller picture of how faience from Nubia changed and developed over time.

The purpose of this pilot study was to examine a small number of samples from a wide time period in order to see how faience found in Nubia could and did change. Of interest here is the observation of glassy faience from the Kerma Period, alongside the high plant ash levels observed, which indicate the use of a mixed-alkali and therefore a specific technological tradition and a more local production. Also of interest—and this is something that raises questions about a potential cross-pollination from glass technology to faience production—is the very high level of lead in one of the samples from the Napatan Period.

What this initial study highlights is the need for further investigation of faience found in Nubia so as to be able to construct a better picture of this industry in a Nubian, rather than in an Egyptian context and how Nubia relates to the wider history of faience and vitreous material production in the ancient world.

Declaration of competing interest

The authors declare that they have no known competing financial interests or personal relationships that could have appeared to influence the work reported in this paper.

Acknowledgments

My thanks to Irit Narkiss and Campbell Price from the Manchester Museum and Gina Criscenzo-Laycock from the Garstang Museum, Liverpool, for allowing access to the material examined here and to the Professor Elizabeth Slater Archaeological Research Laboratories for access to facilities and technical support. My thanks to Matthew Ponting for his comments on a draft of this paper and to the anonymous reviewers and editors. The initial study was made possible by the Arts and Humanities Research Council NorthWest Consortium Doctorial Training Partnership (AHRC NWCDTP), United Kingdom.

Appendix

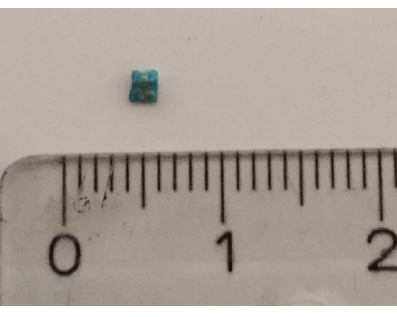
Table A1

Dataset of C-Group 1a samples.

Accession and bead number, and provenance	Date and bibliography	Colour and description	Photographs
MAN8439(a).1 C Group Cemetery 2/132/788, Faras	C-Group Phase 1a (Griffiths, 1921: 72-79)	Pale green/blue exterior. Ring-shaped bead. Evidence of wear on surface.	
MAN8439(a).2 C Group Cemetery 2/132/788, Faras	C-Group Phase 1a (Griffiths, 1921: 72-79)	Pale green/blue exterior. Ring-shaped bead. More evidence of wear on exterior. surface than 8439(a).1.	

Table A2

Dataset of classic kerma period samples.

Accession and bead number, and provenance	Date and bibliography	Colour and description	Photographs
MAN8561.1 Tumulus KX, Kerma	Classic Kerma Period (Reisner, 1923: 96-97 ; see Minor, 2012: 57-60 for dating of tumulus KX)	Bright turquoise exterior and interior. Ring-shaped bead. Shine on exterior surface. Recent break.	
MAN8561.2 Tumulus KX, Kerma	Classic Kerma Period (Reisner, 1923: 96-97 ; see Minor, 2012: 57-60 for dating of tumulus KX)	Bright turquoise exterior and interior. Ring-shaped bead. Shine on exterior surface. Recent break.	

(continued on next page)

Table A2 (continued)

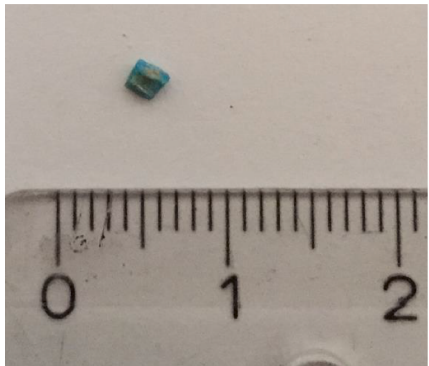
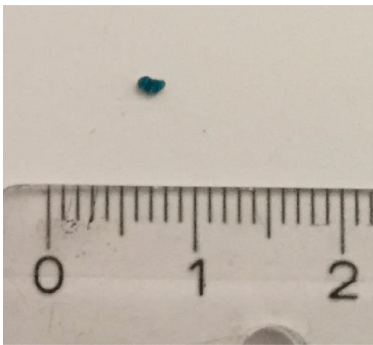
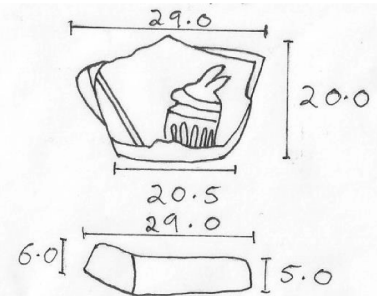
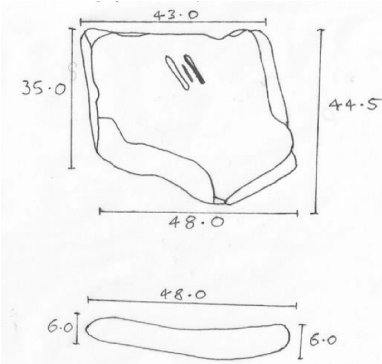
Accession and bead number, and provenance	Date and bibliography	Colour and description	Photographs
MAN8561.3 Tumulus KX, Kerma	Classic Kerma Period (Reisner, 1923: 96-97; see Minor, 2012: 57-60 for dating of tumulus KX)	Bright turquoise exterior and interior. Ring-shaped bead. Shine on exterior surface. Recent break.	
MAN8561.4 Tumulus KX, Kerma	Classic Kerma Period (Reisner, 1923: 96-97; see Minor, 2012: 57-60 for dating of tumulus KX)	Bright turquoise exterior and interior. Ring-shaped bead. Shine on exterior surface. Evidence of deposit on bead. Recent break.	
MAN8561.5 Tumulus KX, Kerma	Classic Kerma Period (Reisner, 1923: 96-97; see Minor, 2012: 57-60 for dating of tumulus KX)	Bright turquoise exterior and interior. Ring-shaped bead. Shine on exterior surface. Recent break.	
MAN8561.6 Tumulus KX, Kerma	Classic Kerma Period (Reisner, 1923: 96-97; see Minor, 2012: 57-60 for dating of tumulus KX)	Bright turquoise exterior and interior. Ring-shaped bead. Shine on exterior surface. Recent break.	

Table A3

Dataset of New Kingdom samples.

Accession and bead number, and provenance	Date and bibliography	Colour and description	Photographs and drawings (measurements given in mm)
MAN8442(a).3 Temple of Hathor, Faras	New Kingdom (Griffiths, 1921: 84-89)	Grey/green exterior. Vessel fragment. Evidence of 'air' bubbles in interior. Evidence of light green/grey coloured decoration on surface. Other surface shows evidence of blackening.	 
MAN8442(b).4 Temple of Hathor, Faras	New Kingdom (Griffiths, 1921: 84-89)	Grey and red/brown exterior. Vessel fragment. Evidence of 'air' bubbles in interior. Evidence of red/brown residue(?) on surface.	 

(continued on next page)

Table A3 (continued)

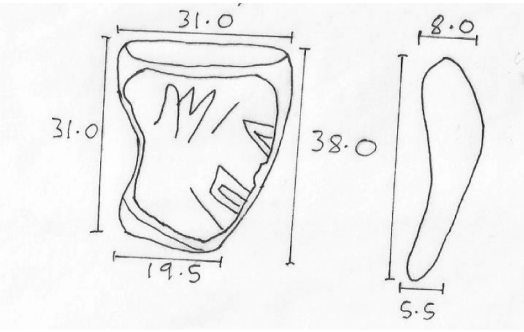
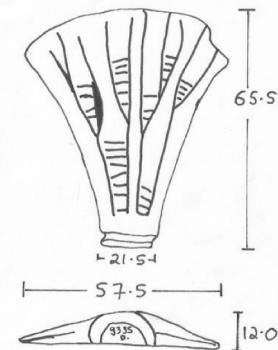
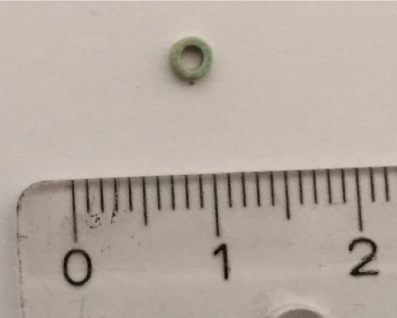
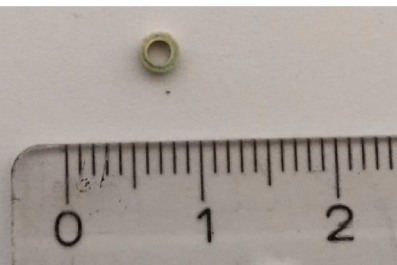
Accession and bead number, and provenance	Date and bibliography	Colour and description	Photographs and drawings (measurements given in mm)
MAN8442(d).5 Temple of Hathor, Faras	New Kingdom (Griffiths, 1921: 84-89)	Light grey exterior of fragment. Light brown/buff interior of fragment. Vessel fragment. Evidence of brown decoration on internal surface.	 

Table A4

Dataset of Middle Napatan Period samples.

Accession and bead number, and provenance	Date and bibliography	Colour and description	Photographs and drawings of inlays (measurements given in mm)
MAN9335(d).1 Temple A, Kawa	Middle Napatan Period (Griffiths, 1922: 79-124)	Buff tone exterior. Darker buff tone interior. Lotus flower inlay (discoloured, evidence of light turquoise colour on surface). Surface cracks visible. 'Air' bubble craters visible on surface. Ancient break.	 
MAN6498.1 Sanam Cemetery, Napata	Middle Napatan Period (Griffiths, 1923)	Pale turquoise exterior. Regular ring-shaped bead. Evidence of wear on exterior surface.	
MAN6498.2 Sanam Cemetery, Napata	Middle Napatan Period (Griffiths, 1923)	Pale turquoise exterior. Regular ring-shaped bead. More evidence of wear on exterior surface than 6498.1.	

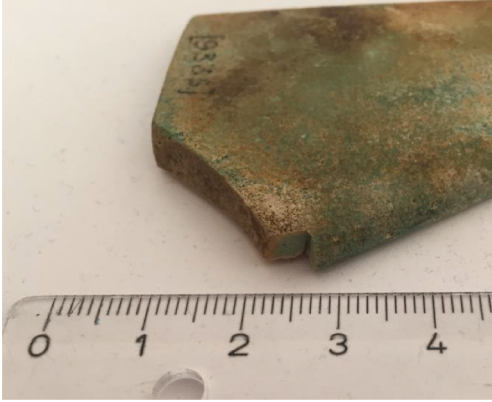
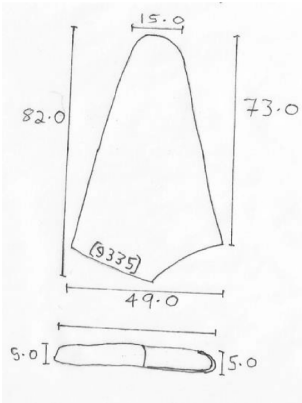
(continued on next page)

Table A4 (continued)

Accession and bead number, and provenance	Date and bibliography	Colour and description	Photographs and drawings of inlays (measurements given in mm)
MAN9341.1 Temple A, Kawa	Middle Napatan Period (Griffiths, 1922: 79–124)	Turquoise exterior. Ring-shaped bead. Evidence of wear on exterior surface.	
MAN9341.2 Temple A, Kawa	Middle Napatan Period (Griffiths, 1922: 79–124)	Turquoise exterior. Ring-shaped bead. More evidence of wear on exterior surface than 9341.1.	
MAN6536-5.1 Sanam Cemetery, N1/1181R/P, infilling, Napata	Middle Napatan Period (Griffiths, 1923: 165)	Turquoise blue exterior and pale turquoise interior. Ring-shaped bead. Residue on outer surface. Interior turquoise blue is of a brighter colour than the exterior. Modern break.	
MAN6536-5.2 Sanam Cemetery, N1/1181R/P, infilling, Napata	Middle Napatan Period (Griffiths, 1923: 165)	Turquoise blue exterior and turquoise interior. Ring-shaped bead. Residue on outer surface. Interior turquoise blue is of a brighter colour than the exterior. Modern break.	

(continued on next page)

Table A4 (continued)

Accession and bead number, and provenance	Date and bibliography	Colour and description	Photographs and drawings of inlays (measurements given in mm)
MAN9335(a-d).1 Kawa	Middle Napatan Period (Griffiths, 1922)	Turquoise blue exterior and interior. Lotus-flower inlay. Severely discoloured. 'Air' bubbles visible on exterior surface. Ancient break. (Angled-notch due to modern sampling.)	   

(continued on next page)

Table A4 (continued)

Accession and bead number, and provenance	Date and bibliography	Colour and description	Photographs and drawings of inlays (measurements given in mm)
MAN6513.1 Sanam Cemetery, N1/727D at neck, Napata	Middle Napatan Period (Griffiths, 1923: 158)	Pale faded turquoise exterior. Pale interior. Melon-shaped bead. Outer surface worn to reveal pale body material. Modern break.	

Table A5.1

Dataset of Meroitic Period samples (Faras).

Accession and bead number, and provenance	Date and bibliography	Colour and description	Photographs
MAN5604.4 Cemetery 1, Grave 2072, (at feet) Faras	Meroitic Period (Griffiths, 1925)	Pale turquoise exterior and interior. Ring-shaped bead. Evidence of heavy wear on exterior surface. Modern break.	
MAN5604.5 Cemetery 1, Grave 2072, (at feet) Faras	Meroitic Period (Griffiths, 1925)	Pale grey exterior and white interior. Ring-shaped bead. Evidence of wear on exterior surface. Modern break	
MAN5608(a).1 Cemetery 1, Grave 693, Faras	Meroitic Period 1st-2nd Century CE (Griffiths, 1925: 103 ; see Spedding, 2023b for details of analysis of glass from this grave)	Pale turquoise exterior and interior. Ring-shaped bead. Evidence of wear on exterior surface. Modern break.	

(continued on next page)

Table A5.1 (continued)

Accession and bead number, and provenance	Date and bibliography	Colour and description	Photographs
MAN5608(a).2 Cemetery 1, Grave 693, Paras	Meroitic Period 1st-2nd Century CE (Griffiths, 1925: 103; see Spedding, 2023b for details of analysis of glass from this grave)	Pale turquoise exterior and interior. Ring-shaped bead. Evidence of wear on exterior surface. Modern break.	

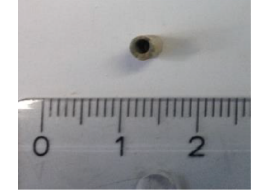
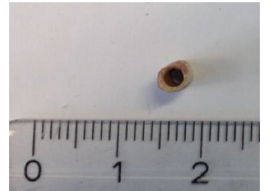
Table A5.2

Dataset of Meroitic Period samples (Meroe).

Accession and bead number, and provenance	Date and bibliography	Colour and description	Photographs
E. 8013.1 Meroe	Meroitic Period (Garstang excavation, see Török, 1997: 9–10 for problems associated with provenances and contexts for material from Garstang's excavations)	Pale green/blue. Ovoid bead. Worn surface where glaze has come away to reveal the body material. Modern break.	 
E.8013.2 Meroe	Meroitic Period (Garstang excavation, see Török, 1997: 9–10 for problems associated with provenances and contexts for material from Garstang's excavations)	Green/blue. Cylindrical bead. Evidence of slight wear on the surface removing glaze to reveal body material beneath.	 

(continued on next page)

Table A5.2 (continued)

Accession and bead number, and provenance	Date and bibliography	Colour and description	Photographs
E.8063.1 Meroe	Meroitic Period (Garstang excavation, see Török, 1997: 9–10 for problems associated with provenances and contexts for material from Garstang's excavations)	Pale green/blue. Cylindrical bead. Slightly worn surface to reveal body material in places. Very thin walls. Evidence of break.	 
E.8063.2 Meroe	Meroitic Period (Garstang excavation, see Török, 1997: 9–10 for problems associated with provenances and contexts for material from Garstang's excavations)	Very pale green/blue. Cylindrical bead. Worn surface to reveal body material beneath. Evidence of break.	 
E.8063.3 Meroe	Meroitic Period (Garstang excavation, see Török, 1997: 9–10 for problems associated with provenances and contexts for material from Garstang's excavations)	Red/brown. Cylindrical bead. Very worn surface to reveal body material beneath. Evidence of break.	  

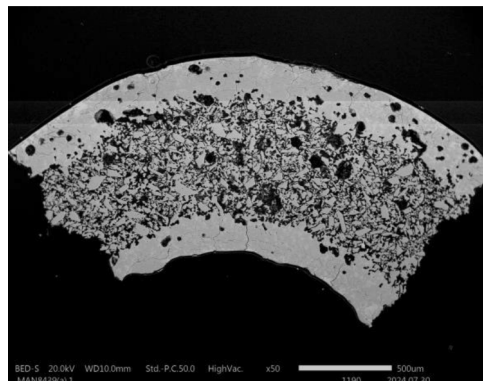
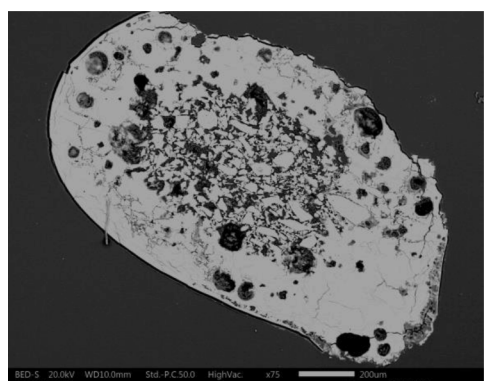
(continued on next page)

Table A5.2 (continued)

Accession and bead number, and provenance	Date and bibliography	Colour and description	Photographs
E.8070.1 Meroe	Meroitic Period (Garstang excavation, see Török, 1997: 9–10 for problems associated with provenances and contexts for material from Garstang's excavations)	Green/blue. Spherical bead. Evidence of wear on the surface to reveal the body material beneath. Hole goes through body at an angle.	

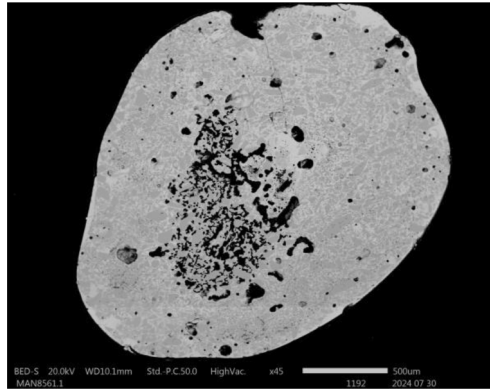
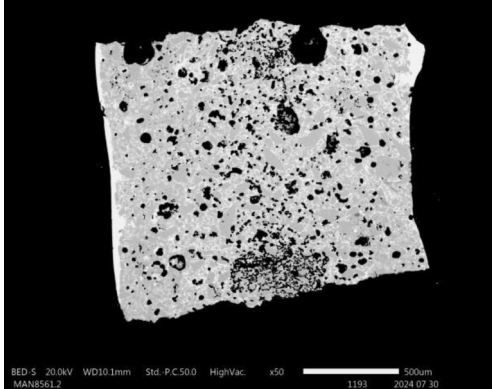
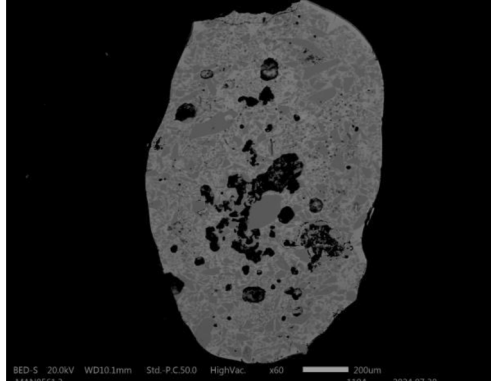
Table A6

All BSE images of samples analysed here.

Accession and sample no.	Site	Context	Date	Backscatter electron image
MAN8439(a).1	Faras	C-Group Cemetery	C-Group 1a	 BED S 20.0kV WD10.0mm Std -P.C50.0 HighVac. x50 1190 500μm MAN8439(a).1 2024 07 30
MAN8439(a).2	Faras	C-Group Cemetery	C-Group 1a	 BED S 20.0kV WD10.0mm Std -P.C50.0 HighVac. x75 1191 200μm MAN8439(a).2 2024 07 30

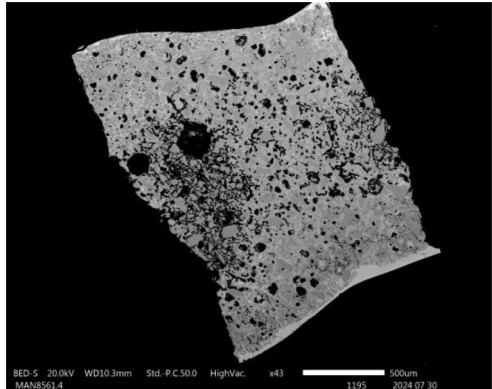
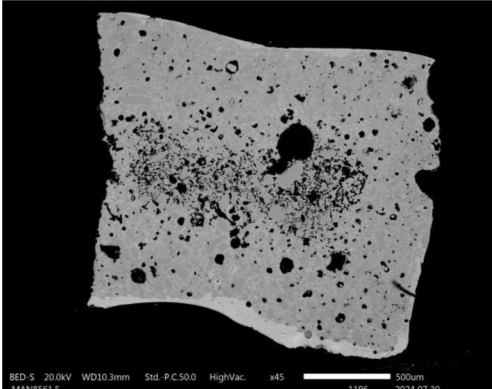
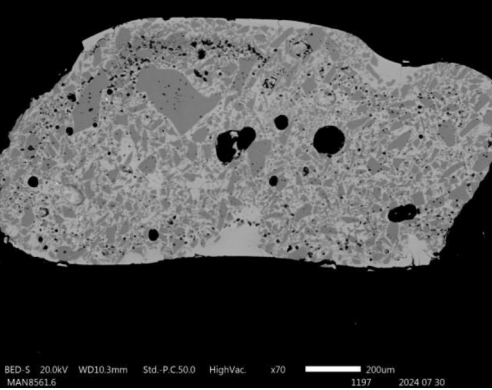
(continued on next page)

Table A6 (continued)

Accession and sample no.	Site	Context	Date	Backscatter electron image
MAN8561.1	Kerma	Tumulus KX	Classic Kerma Period	 <p>BED-S 20.0kV WD10.1mm Std.-P.C.50.0 HighVac. x65 MAN8561.1 1192 500μm 2024.07.30</p>
MAN8561.2	Kerma	Tumulus KX	Classic Kerma Period	 <p>BED-S 20.0kV WD10.1mm Std.-P.C.50.0 HighVac. x50 MAN8561.2 1193 500μm 2024.07.30</p>
MAN8561.3	Kerma	Tumulus KX	Classic Kerma Period	 <p>BED-S 20.0kV WD10.1mm Std.-P.C.50.0 HighVac. x60 MAN8561.3 1194 200μm 2024.07.30</p>

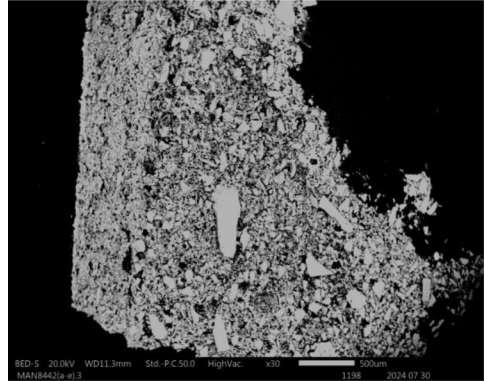
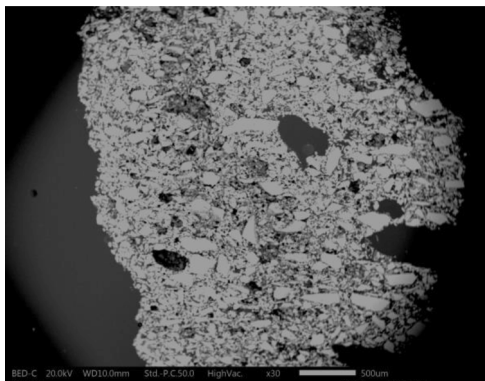
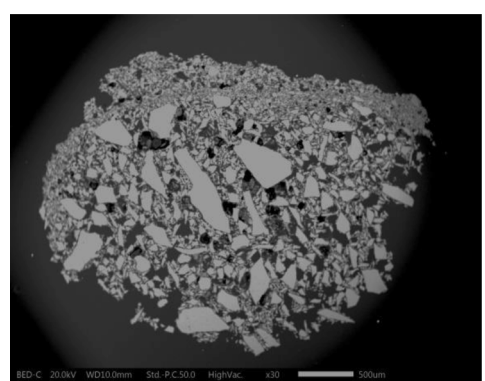
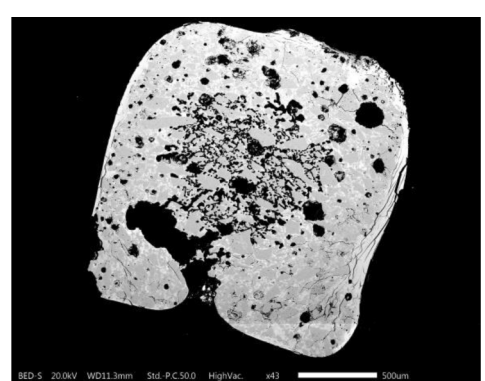
(continued on next page)

Table A6 (continued)

Accession and sample no.	Site	Context	Date	Backscatter electron image
MAN8561.4	Kerma	Tumulus KX	Classic Kerma Period	 <p>BED-S 20.0kV WD10.3mm Std.-P.C.50.0 HighVac. x43 MAN8561.4 1195 2024 07 30 500μm</p>
MAN8561.5	Kerma	Tumulus KX	Classic Kerma Period	 <p>BED-S 20.0kV WD10.3mm Std.-P.C.50.0 HighVac. x45 MAN8561.5 1196 2024 07 30 500μm</p>
MAN8561.6	Kerma	Tumulus KX	Classic Kerma Period	 <p>BED-S 20.0kV WD10.3mm Std.-P.C.50.0 HighVac. x70 MAN8561.6 1197 2024 07 30 200μm</p>

(continued on next page)

Table A6 (continued)

Accession and sample no.	Site	Context	Date	Backscatter electron image
MAN8442(a-e).3	Faras	Temple of Hathor	New Kingdom	
MAN8442(a-e).4	Faras	Temple of Hathor	New Kingdom	
MAN8442(a-e).5	Faras	Temple of Hathor	New Kingdom	
MAN9341.1	Kawa	Temple A	Middle Napatan Period	

(continued on next page)

Table A6 (continued)

Accession and sample no.	Site	Context	Date	Backscatter electron image
MAN9341.2	Kawa	Temple A	Middle Napatan Period	
MAN9335(a-d).1	Kawa	Kawa	Middle Napatan Period	
MAN9335(d).1	Kawa	Kawa	Middle Napatan Period	
MAN6498.1	Sanam	Cemetery	Middle Napatan Period	

(continued on next page)

Table A6 (continued)

Accession and sample no.	Site	Context	Date	Backscatter electron image
MAN6498.2	Sanam	Cemetery	Middle Napatan Period	<p>BED-S 20.0kV WD10.8mm Std.-P.C50.0 HighVac. x45 1203 500um 2024.07.31</p>
MAN6513.1	Sanam	Cemetery, N1/727D	Middle Napatan Period	<p>BED-S 20.0kV WD10.8mm Std.-P.C50.0 HighVac. x40 1204 500um 2024.07.31</p>
MAN6536-5.1	Sanam	Cemetery, N1/1181R/P	Middle Napatan Period	<p>BED-S 20.0kV WD10.8mm Std.-P.C50.0 HighVac. x30 1206 500um 2024.07.31</p>

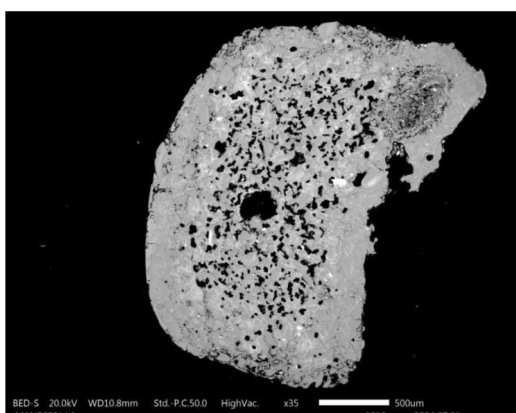
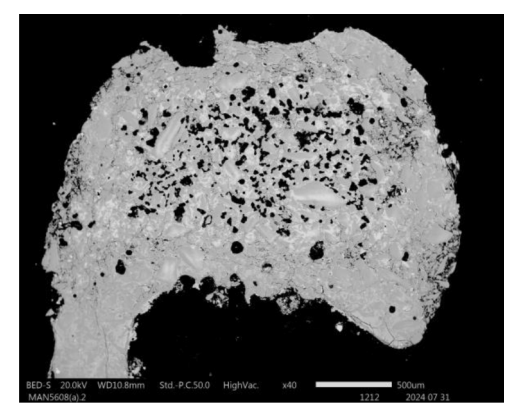
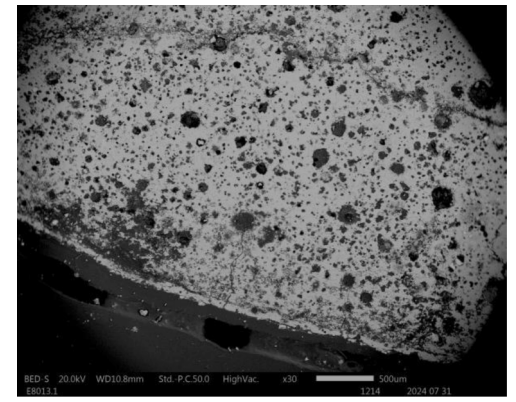
(continued on next page)

Table A6 (continued)

Accession and sample no.	Site	Context	Date	Backscatter electron image
MAN6536-5.2	Sanam	Cemetery, N1/1181R/P	Middle Napatan Period	
MAN5604.4	Paras	Cemetery 1, Grave 2072	Meroitic Period	
MAN5604.5	Paras	Cemetery 1, Grave 2072	Meroitic Period	

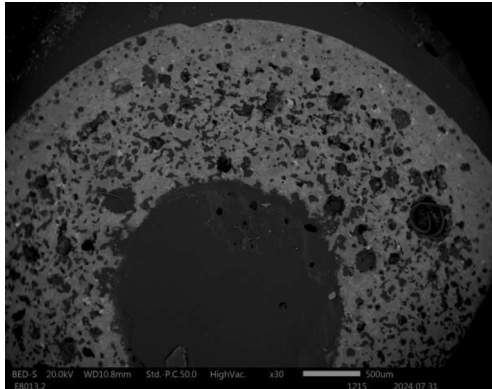
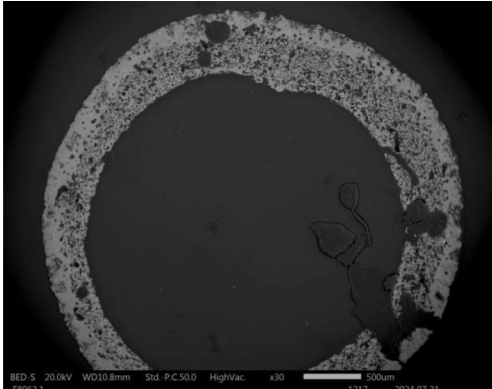
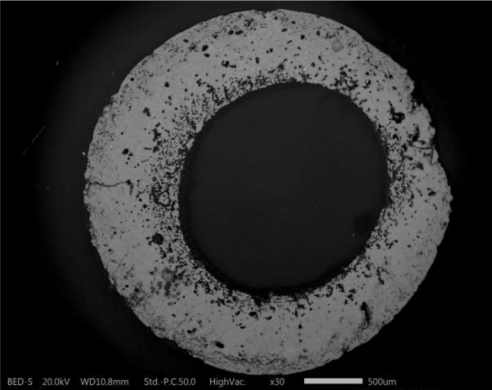
(continued on next page)

Table A6 (continued)

Accession and sample no.	Site	Context	Date	Backscatter electron image
MAN5608(a).1	Faras	Cemetery 1, Grave 693	Meroitic Period (1st-2nd century CE)	
MAN5608(a).2	Faras	Cemetery 1, Grave 693	Meroitic Period (1st-2nd century CE)	
E.8013.1	Meroe	Meroe	Meroitic Period	

(continued on next page)

Table A6 (continued)

Accession and sample no.	Site	Context	Date	Backscatter electron image
E.8013.2	Meroe	Meroe	Meroitic Period	
E.8063.1	Meroe	Meroe	Meroitic Period	
E.8063.2	Meroe	Meroe	Meroitic Period	

(continued on next page)

Table A6 (continued)

Accession and sample no.	Site	Context	Date	Backscatter electron image
E.8063.3	Meroe	Meroe	Meroitic Period	
E.8070.1	Meroe	Meroe	Meroitic Period	

Table A7

Non-normalised results in wt% for Napatan to Meroitic Period Samples (ND indicates not detected when a value of 0.00 wt% was given).

NAPATAN															
MAN9335.1															
Faience component	Na ₂ O	MgO	Al ₂ O ₃	SiO ₂	K ₂ O	CaO	TiO ₂	MnO	Fe ₂ O ₃	CoO	CuO	Sb ₂ O ₅	PbO	Total	
Glaze layer	0.25	ND	0.41	57.70	0.26	0.59	0.04	ND	0.32	0.03	4.07	0.30	0.32	64.31	
Body	0.04	ND	0.23	61.91	0.14	0.15	0.01	0.01	0.13	ND	0.95	0.05	0.35	63.97	
MAN6498.1														TOTAL	
Glaze layer	Na ₂ O	MgO	Al ₂ O ₃	SiO ₂	K ₂ O	CaO	TiO ₂	MnO	Fe ₂ O ₃	CoO	CuO	Sb ₂ O ₅	PbO		
Interaction layer	0.44	ND	1.11	73.00	0.07	0.13	0.06	ND	0.10	0.01	1.09	0.02	0.20	76.26	
Body	ND	ND	0.52	65.66	0.20	0.12	0.01	ND	0.25	0.02	0.75	ND	ND	67.53	
MAN6498.2														TOTAL	
Glaze layer	Na ₂ O	MgO	Al ₂ O ₃	SiO ₂	K ₂ O	CaO	TiO ₂	MnO	Fe ₂ O ₃	CoO	CuO	Sb ₂ O ₅	PbO		
Interaction layer	0.49	ND	1.30	79.60	0.21	0.17	0.03	ND	0.35	0.02	0.44	0.04	ND	82.64	
Body	2.32	ND	1.52	85.57	0.90	0.32	0.08	0.01	0.87	ND	1.20	0.36	0.48	93.63	
MAN6513.1														TOTAL	
Glaze layer	Na ₂ O	MgO	Al ₂ O ₃	SiO ₂	K ₂ O	CaO	TiO ₂	MnO	Fe ₂ O ₃	CoO	CuO	Sb ₂ O ₅	PbO		
Interaction layer	0.10	ND	0.51	54.89	0.01	0.47	0.17	0.02	2.24	ND	1.04	0.05	15.95	75.47	
Body	3.34	ND	1.48	77.08	1.42	0.14	0.02	0.02	3.28	0.04	0.12	0.44	5.81	93.19	
MAN6536-5.1														TOTAL	
Glaze layer	Na ₂ O	MgO	Al ₂ O ₃	SiO ₂	K ₂ O	CaO	TiO ₂	MnO	Fe ₂ O ₃	CoO	CuO	Sb ₂ O ₅	PbO		
Interaction layer	0.83	ND	1.49	71.94	0.35	0.66	0.03	0.11	0.32	0.03	3.00	0.16	ND	68.32	
MAN6536-5.2														TOTAL	
Glaze layer	Na ₂ O	MgO	Al ₂ O ₃	SiO ₂	K ₂ O	CaO	TiO ₂	MnO	Fe ₂ O ₃	CoO	CuO	Sb ₂ O ₅	PbO		
Body	0.46	ND	0.60	71.61	0.06	2.02	0.04	0.07	0.47	0.01	10.27	0.10	0.58	86.32	
MEROITIC														TOTAL	
MAN5604.4															

(continued on next page)

Table A7 (continued)

NAPATAN														
	Na ₂ O	MgO	Al ₂ O ₃	SiO ₂	K ₂ O	CaO	TiO ₂	MnO	Fe ₂ O ₃	CoO	CuO	Sb ₂ O ₅	PbO	TOTAL
Glaze layer Body MAN5604.5	0.01	ND	0.06	81.43	ND	0.05	0.02	0.02	0.02	ND	0.22	0.03	0.04	81.91
	0.05	ND	0.27	52.22	0.11	0.16	0.04	0.04	0.21	0.04	1.00	0.09	0.05	54.30
	Na ₂ O	MgO	Al ₂ O ₃	SiO ₂	K ₂ O	CaO	TiO ₂	MnO	Fe ₂ O ₃	CoO	CuO	Sb ₂ O ₅	PbO	TOTAL
Glaze layer Body MAN5608(a).1	1.79	12.52	9.44	39.66	0.78	5.41	0.51	0.05	5.50	0.01	5.73	0.08	0.05	81.56
	ND	ND	0.25	54.72	0.11	2.47	0.01	0.01	0.45	0.04	0.38	ND	0.13	58.58
	Na ₂ O	MgO	Al ₂ O ₃	SiO ₂	K ₂ O	CaO	TiO ₂	MnO	Fe ₂ O ₃	CoO	CuO	Sb ₂ O ₅	PbO	TOTAL
Glaze layer Interaction layer Body MAN5608(a).2	0.61	0.02	0.58	66.30	0.01	1.18	0.025	0.06	0.13	ND	3.74	ND	1.10	73.75
	0.58	ND	1.12	74.39	0.15	0.61	0.07	ND	0.58	0.02	1.40	0.10	0.75	79.77
	1.48	0.05	0.56	69.51	0.36	0.74	0.07	0.01	0.47	ND	0.92	0.05	0.49	74.70
Body E.8013.1	Na ₂ O	MgO	Al ₂ O ₃	SiO ₂	K ₂ O	CaO	TiO ₂	MnO	Fe ₂ O ₃	CoO	CuO	Sb ₂ O ₅	PbO	TOTAL
	1.34	ND	0.59	84.57	0.48	1.28	0.08	ND	0.54	0.08	1.06	0.11	0.34	90.49
	Na ₂ O	MgO	Al ₂ O ₃	SiO ₂	K ₂ O	CaO	TiO ₂	MnO	Fe ₂ O ₃	CoO	CuO	Sb ₂ O ₅	PbO	TOTAL
Glaze layer Body E.8013.2	0.05	0.04	ND	69.11	0.04	0.75	ND	ND	0.32	ND	0.49	ND	0.24	71.05
	0.15	0.09	0.03	58.00	0.09	0.83	0.02	ND	0.38	0.03	0.24	0.04	ND	59.90
	Na ₂ O	MgO	Al ₂ O ₃	SiO ₂	K ₂ O	CaO	TiO ₂	MnO	Fe ₂ O ₃	CoO	CuO	Sb ₂ O ₅	PbO	TOTAL
Glaze layer Body E.8070.1	0.81	1.10	0.37	62.14	0.22	0.97	0.01	0.01	0.30	0.08	5.51	0.09	0.28	71.92
	1.12	0.16	0.06	66.36	0.26	1.31	0.01	0.03	0.22	ND	1.98	0.82	0.43	72.78
	Na ₂ O	MgO	Al ₂ O ₃	SiO ₂	K ₂ O	CaO	TiO ₂	MnO	Fe ₂ O ₃	CoO	CuO	Sb ₂ O ₅	PbO	TOTAL
Glaze layer Body E.8063.1	0.11	0.06	0.01	68.32	0.16	0.61	0.01	0.01	0.13	ND	0.20	ND	0.07	69.72
	0.07	0.10	0.02	44.81	0.14	2.34	0.01	0.01	0.15	ND	0.02	ND	ND	47.69
	Na ₂ O	MgO	Al ₂ O ₃	SiO ₂	K ₂ O	CaO	TiO ₂	MnO	Fe ₂ O ₃	CoO	CuO	Sb ₂ O ₅	PbO	TOTAL
Glaze layer Body E.8063.2	ND	ND	0.61	74.73	0.53	0.22	0.03	0.03	0.27	0.03	1.43	0.07	ND	77.96
	0.06	0.03	0.18	53.42	0.24	0.2	0.03	ND	0.09	ND	0.39	ND	ND	54.67
	Na ₂ O	MgO	Al ₂ O ₃	SiO ₂	K ₂ O	CaO	TiO ₂	MnO	Fe ₂ O ₃	CoO	CuO	Sb ₂ O ₅	PbO	TOTAL
Glaze layer Body E.8063.3	ND	0.01	0.01	70.35	0.06	0.05	0.01	0.01	0.01	ND	0.10	0.05	0.02	70.68
	ND	ND	0.03	78.75	0.23	0.22	0.01	0.01	0.54	0.02	1.48	0.19	0.31	81.8
	Na ₂ O	MgO	Al ₂ O ₃	SiO ₂	K ₂ O	CaO	TiO ₂	MnO	Fe ₂ O ₃	CoO	CuO	Sb ₂ O ₅	PbO	TOTAL
Glaze layer Body	ND	0.18	ND	76.00	0.15	0.32	0.01	0.01	0.41	0.01	0.04	0.06	ND	77.21
	0.06	ND	0.30	48.41	0.20	0.45	ND	0.03	0.29	0.03	0.08	0.01	0.17	50.05

Data availability

Data will be made available on request.

References

- Adlington, L.W., 2017. The corning archaeological reference glasses: new values for "old" compositions. *Papers Inst. Archaeol.* 27, 1–8.
- Barber, D.J., Freestone, I.C., Moulding, K.M., 2009. Ancient Copper Red Glasses: Investigation and Analysis by Microbeam Techniques. In: Shortland, A.J., Freestone, I.C., Rehren, Th. (Eds.), *From Mine to Microscope: Advances in the Study of Ancient Technology*. Oxbow Books, Oxford, pp. 115–127.
- Dal Bianco, B., Bertoncello, R., Milanese, L., Barison, S., 2005. Glass corrosion across the alps: a surface study of chemical corrosion of glasses found in marine and ground environments. *Archaeometry* 47, 351–360.
- van Elteren, J.T., Izmer, A., Sala, M., Orsega, E.F., Selih, V.S., Panighello, S., Vanhaecke, F., 2013. 3D laser ablation-ICP-mass spectrometry mapping for the study of surface layer phenomena – a case study for weathered glass. *J. Anal. Atomic Spectrometry* 28, 994–1004.
- Freestone, I.C., Stapleton, C.P., Rigby, V., 2003. The production of red glass and enamel in the late iron age, roman and byzantine periods. In: Entwistle, C. (Ed.), *Through a Glass Brightly: Studies in Byzantine and Medieval Art and Archaeology Presented to David Buckton*. Oxbow Books, Oxford, pp. 142–154.
- Gatto, M.C., 2011. The relative chronology of Nubia. *Archéo-Nil* 21, 81–100.
- Gentaz, L., Lombardo, T., Chabas, A., Loisel, C., Verney-Carron, A., 2012. Impact of Neocrystallisations on the SiO₂-K₂O-CaO glass degradation due to atmospheric dry depositions. *Atmospheric Environ.* 55, 459–466.
- Griffith, F.L., 1921. Oxford University Excavations in Nubia. *Univ. Liverpool Annals Archaeol. Anthropol.* 8, 1–65.
- Griffith, F.L., 1922. Oxford University Excavations in Nubia. *Univ. Liverpool Annals Archaeol. Anthropol.* 9, 67–124.
- Griffith, F.L., 1923. Oxford Excavations in Nubia XVIII–XXV. The Cemetery of Napata, Sanam. *Univ. Liverpool Annals Archaeol. Anthropol.* 10, 73–171.
- Griffith, F.L., 1924. Oxford Excavations in Nubia XXX–XXXII. The Meroitic Cemetery at Faras. *Univ. Liverpool Annals Archaeol. Anthropol.* 11, 115–125, 141–180.
- Griffith, F.L., 1925. Oxford Excavations in Nubia XXXIV. Classification of the Meroitic Graves at Faras. *Univ. Liverpool Annals Archaeol. Anthropol.* 12, 57–172.
- Griffith, F.L., 1926. Oxford Excavations in Nubia. *Univ. Liverpool Annals Archaeol. Anthropol.* 13, 17–37.
- Hammerle, E., 2011. New technology or regression? A compositional study of faience beads from two tombs in abydos. In: Corbelli, J., Boatright, D., Malleson, C. (Eds.), *Current Research in Egyptology 2009*. Oxbow Books, Oxford, pp. 67–80.
- Hench, L.L., Clark, D.E., 1978. Physical chemistry of glass surfaces. *J. Non-Crystalline Solids* 28, 83–105.
- Kaczmarczyk, A., Hedges, R.E.M., 1983. Ancient Egyptian Faience: An Analytical Survey of Egyptian Faience from Predynastic to Roman Times. Aris & Phillips, Warminster.
- Lacovara, P., 2021. The Faience Industry at Kerma. *J. Ancient Egypt. Interc.* 29, 32–38.
- Lacovara, P., 2024. Nubian faience. In: Budka, J., Lemos, R. (Eds.), *Landscape and Resource Management in Bronze Age Nubia*. Harrassowitz Verlag, Wiesbaden, pp. 47–56.
- Lemos, R., 2024. Nubian material resources between indigenous diversity and colonial impositions. In: Budka, J., Lemos, R. (Eds.), *Landscape and Resource Management in Bronze Age Nubia*. Harrassowitz Verlag, Wiesbaden, pp. 201–205.
- Lucas, A., Harris, J.R., 1962. *Ancient Egyptian Materials and Industries*, fourth ed. Dover, London.
- Matin, M., Matin, M., 2012. Egyptian faience glazing by the cementation method part 1: an investigation of the glazing powder composition and glazing mechanism. *J. Archaeol. Sci.* 39, 763–776.
- Matin, M., Matin, M., 2016. Egyptian faience glazing by the cementation method part 2: cattle dung ash as a possible source of alkali flux. *Archaeol. Anthropol. Sci.* 8, 125–134.
- Minor, E., 2012. The Use of Egyptian and Egyptianizing Material Culture in Nubian Burials of the Classic Kerma Period. Unpublished PhD dissertation.
- Minor, E., 2014. The use of Egyptian and Egyptianizing Material Culture in Classic Kerma Burials: Winged Sun Discs. In: Feldman, M., Casanova, C. (Eds.), *Luxury Goods: Production, Exchange, and Heritage in the near East during the Bronze and Iron Ages*. De Boccard Publishing, Paris, pp. 225–234.

- Munier, I., Lefevre, R.A., Losno, R., 2002. Atmospheric Factors Influencing the Formation of Neocrystallisations on low durability glass exposed to urban atmosphere. *Glass Technol.: Eur J. Glass Sci. Technol. Part A* 43, 114–124.
- Newbury, D.E., Ritchie, N.W.M., 2015. Performing elemental microanalysis with high accuracy and high precision by scanning electron microscopy/silicon drift detector energy-dispersive X-ray spectrometry (SEM/SDD-EDS). *J. Mater. Sci.* 50, 493–518.
- Nicholson, P.T., Peltenburg, E., Egyptian Faience, 2009. In: Nicholson, P.T., Shaw, I. (Eds.), *Ancient Egyptian Materials and Technology*. Cambridge University Press, Cambridge, pp. 177–194.
- Panighello, S., van Elteren, J.T., Orsega, E.F., Moretoo, L.M., 2015. Laser ablation-ICP-MS depth profiling to study ancient glass surface degradation. *Anal. Bioanal. Chem.* 407, 3377–3391.
- Reisner, G.A., 1923. Excavations at Kerma Parts IV-V, Harvard African Studies. Peabody Museum Press, Cambridge.
- Rehren, Th., 2008. A review of factors affecting the composition of early Egyptian glasses and faience: Alkali and Alkali Earth Oxides. *J. Archaeol. Sci.* 35, 1345–1354.
- Rehren, Th., Freestone, I.C., 2015. Ancient glass: from kaleidoscope to crystal ball. *J. Archaeol. Sci.* 56, 233–241.
- Rehren, Th., Connolly, P., Schibille, N., Schwärzer, H., 2015. Changes in glass consumption in pergamon (Turkey) from hellenistic to late byzantine and Islamic times. *J. Archaeol. Sci.* 55, 266–279.
- Rosenow, D., Rehren, Th., 2014. Herding cats – roman to late antique glass groups from bastis, Northern Egypt. *J. Archaeol. Sci.* 49, 170–184.
- Schibille, N., 2011. Supply routes and the consumption of glass in first millennium CE Butrint (Albania). *J. Archaeol. Sci.* 38, 2939–2948.
- Shortland, A.J., Eremin, K., 2006. The analysis of second millennium glass from Egypt and mesopotamia, Part 1: new WDS analysis. *Archaeometry* 48, 581–603.
- Smith, S.T., Buzon, M.R., (2017). Colonial Encounters at New Kingdom Tombs: Cultural Entanglements and Hybrid Identity, in: Spencer, N., Stevens, A., Binder, M. (eds.), *Nubia in the New Kingdom: Lived Experience, Pharaonic Control and Indigenous Traditions*. Peeters, Leuven, 615–630.
- Smith, S.T., 2022. "Backwater Puritans"? Racism, Egyptological Stereotypes, and Cosmopolitan Society at Kushite Tombs. *J. Ancient Egypt. Interc.* 35, 190–217.
- Spedding, J.V., 2018. A Preliminary Analytical Investigation of Nubian Glass of the Meroitic Period. In: Tipper, S., Tully, G. (Eds.), *Current Research in Nubian Archaeology*. Gorgias Press, Piscataway, pp. 37–81.
- Spedding, J.V., 2022. Lead isotope analysis of meroitic period glass from Nubia with LA-MC-ICP-MS. *Archaeometry* 64, 1148–1167. <https://doi.org/10.1111/arcm.12780>.
- Spedding, J.V., 2023a. SEM-EDS identification of glass groups in meroitic-period and early-Nobadian Nubia. *Azania: Archaeol. Res. Africa* 57, 500–531. <https://doi.org/10.1080/0067270X.2022.2157624>.
- Spedding, J.V., 2023b. "To see a world in a grain of sand": glass from Nubia and the ancient mediterranean. Archaeopress, Oxford. <https://doi.org/10.2307/jj.3452817>.
- Spedding, J.V., Forthcoming. A Brittle Glass: The Influence of Lead in Ancient Glasses on Glass Decay.
- Stocks, D.A., 1997. Derivation of ancient Egyptian faience core and glaze materials. *Antiquity* 71, 179–182.
- Tite, M.S., Freestone, I.C., Bimson, M., 1983. Egyptian faience: an investigation of the methods of production. *Archaeometry* 25, 17–27.
- Tite, M.S., Shortland, A.J., 2008. Production Technology of Faience and Related Early Vitreous Materials. Oxford University School of Archaeology, Oxford.
- Török, L., 1997. Meroe City an Ancient African Capital: John Garstang's Excavations in the Sudan. Egypt Exploration Society, London.
- Török, L., 2009. Between Two Worlds: The Frontier Region between Ancient Nubia and Egypt 3700BC-500AD. Brill, Leiden.
- Tournié, A., Ricciardi, P., Colombari, Ph., 2008. Glass corrosion mechanisms: a multiscale analysis. *Solid State Ion.* 179, 2142–2154.
- Vandiver, P., 1982. Technological Change in Egyptian Faience. In: Olin, J.S., Franklin, A. D. (Eds.), *Archaeological Ceramics*. Smithsonian Institution Press, Washington, pp. 167–179.
- Vilarigues, M., da Silva, R.C., 2009. The effect of Mn, Fe and Cu Ions on Potash-Glass Corrosion. *J. of Non-Crystalline Solids* 355, 1630–1637.
- Won-In, K., Thongkam, Y., Intarasiri, S., Kamwanna, T., Dararutana, P., 2012. Corrosion of ancient glass beads found in Southern Thailand. *Materials Sci. and Eng.* 37, 1–5.